

Signal Processing on Graphs: Causal Modeling of Big Data

Jonathan Mei and José M. F. Moura

Abstract—Often, *Big Data* applications collect a large number of time series, for example, the financial data of companies quoted in a stock exchange, the health care data of all patients that visit the emergency room of a hospital, or the temperature sequences continuously measured by weather stations across the US. A first task in the analytics of these data is to derive a low dimensional representation, a graph or discrete manifold, that describes well the *interrelations* among the time series and their *intrarelations* across time. This paper presents a computationally tractable algorithm for estimating this graph structure from the available data. This graph is directed and weighted, possibly representing causal relations, not just reciprocal correlations as in many existing approaches in the literature. A detailed convergence analysis is carried out. The algorithm is demonstrated on random graph and real network time series datasets, and its performance is compared to that of related methods. The adjacency matrices estimated with the new method are close to the true graph in the simulated data and consistent with prior physical knowledge in the real dataset tested.

Keywords: Graph Signal Processing, Graph Structure, Adjacency Matrix, Network, Time Series, Big Data, Causal

I. INTRODUCTION

There is an explosion of data, generated, measured, and stored at very fast rates in many disciplines, from finance and social media to geology and biology. Much of this *Big Data* takes the form of simultaneous, long running time series. Examples, among many others, include protein-to-protein interactions in organisms, patients records in health care, customers consumptions in (power, water, natural gas) utility companies, cell phone usage for wireless service providers, companies financial data, social interactions among individuals in a population. The internet-of-things (IoT) is an imminent source of ever increasing large collection of time series.

Networks or graphs are becoming prevalent as models to describe data relationships. These low-dimensional graph representations are used for further analytics, for example, to compute statistics, make inferences, perform signal processing tasks [1], [2], [3], or quantify how topology influences diffusion in networks of agents [4]. These methods all use the structure of the *known* graphs to extract knowledge and meaning from the observed data supported on the graphs.

However, in many problems the graph structure itself may be *unknown*, and the first issue to address is inferring the unknown relations between entities from the data. The diversity and *unstructured* nature of Big Data challenges our

ability to derive models from first principles; in alternative, because data is abundant, it is of great significance to develop methodologies that, in collaboration with domain experts, assist extracting low-dimensional representations for the data. Early work in estimating low-dimensional graph-like structure includes dimensionality reduction approaches such as [5], [6]. These methods work on a static snapshot of data and do not incorporate the notion of time.

This paper focuses on finding a graph that describes time series data, estimating the network structure in the form of a possibly directed, weighted adjacency matrix \mathbf{A} . Current work on estimating network structure largely associates graph structure with assuming that the process supported by the graph is Markov along the edges [7], [8] or aims to recover causality [9] in the sense popularized by Granger [10]. Our work instead associates the graph with causal network effects, drawing inspiration from the Discrete Signal Processing on Graphs (DSP_G) framework [3], [11].

We first provide a brief overview of the concepts and notations underlying the DSP_G theory in section II. Then we introduce related prior work in section III and our new network process in section IV. Next, we present algorithms to infer the network structure from data generated by such processes in section V. We provide analysis on the convergence of our algorithms and the performance of the models for prediction in section VI. Finally, we show simulation results in section VII and conclude the paper in section VIII.

II. DISCRETE SIGNAL PROCESSING ON GRAPHS

DSP_G provides a framework with which to analyze data supported on N elements for which relational information between the elements is known. We follow [3], [11] in this brief review.

A. Graph Signals

Consider a graph $G = (\mathbf{V}, \mathbf{A})$ where the vertex set $\mathbf{V} = \{v_0, \dots, v_{N-1}\}$ and \mathbf{A} is the weighted adjacency matrix of the graph. Each data element corresponds to a node v_n , and weight $\mathbf{A}_{n,m}$ is assigned to a directed edge from v_m to v_n . A graph signal is defined as a map

$$\begin{aligned} \mathbf{x} : \mathbf{V} &\rightarrow \mathbb{C} \\ v_n &\mapsto x_n \end{aligned}$$

Since signals are isomorphic to complex vectors with N elements, we can write graph signals as N length vectors supported on \mathbf{V} ,

$$\mathbf{x} = (x_0 \ x_1 \ \dots \ x_{N-1})^T \in \mathbb{C}^N$$

The authors are with the Department of Electrical and Computer Engineering, Carnegie Mellon University, Pittsburgh, PA 15213, USA. ph: (412)268-6341; fax: (412)268-3890; e-mails: [jmei1,moura]@ece.cmu.edu.

This work was partially funded by NSF grants CCF 1011903 and CCF 1513936.

B. Graph Filters

A graph filter is a system $\mathbf{H}(\cdot)$ that takes a graph signal \mathbf{x} as input and outputs another graph signal $\tilde{\mathbf{x}} = \mathbf{H}(\mathbf{x})$. A basic nontrivial graph filter on graph $G = (\mathbf{V}, \mathbf{A})$ called the graph shift is a local operation given by the product of the input signal with the adjacency matrix $\tilde{\mathbf{x}} = \mathbf{A}\mathbf{x}$. Assuming shift invariance, graph filters in DSP_G are matrix polynomials of the form

$$h(\mathbf{A}) = h_0\mathbf{I} + h_1\mathbf{A} + \dots + h_L\mathbf{A}^L$$

The output of the filter is $\tilde{\mathbf{x}} = \mathbf{H}(\mathbf{x}) = h(\mathbf{A})\mathbf{x}$. Note that graph filters are linear shift-invariant filters. For a linear combination of graph signal inputs they produce the same linear combination of graph signal outputs, and consecutive application of multiple graph filters does not depend on the order of application (i.e., graph filters commute). Graph filters also have at most $L \leq N_{\mathbf{A}}$ taps h_ℓ , where $N_{\mathbf{A}} = \deg m_{\mathbf{A}}(z)$ is the degree of the minimal polynomial $m_{\mathbf{A}}(z)$ of \mathbf{A} .

III. RELATION TO PRIOR WORK

Here we describe previous models and methods used to estimate graph structure, noting the similarities and distinctions with the method presented in this paper. In particular, in section III-A we consider sparse Gaussian graphical model selection, in section III-B we consider sparse vector autoregression, and in section III-C we discuss other graph signal processing approaches and our choice of using the adjacency matrix as a shift.

A. Sparse Graphical Model Selection

Sparse inverse covariance estimation [12], [13], [8] combines the Markov property with the assumption of Gaussianity to learn a graph structure describing symmetric relations between the variables. A typical formulation of sparse inverse covariance estimation is Graphical Lasso [12]. Suppose the data matrix representing all the observations is given,

$$\mathbf{X} = (\mathbf{x}[0] \quad \mathbf{x}[1] \quad \dots \quad \mathbf{x}[K-1]) \in \mathbb{R}^{N \times K} \quad (1)$$

In this problem, the data is assumed to be Gaussian, i.e., each $\mathbf{x}[i] \sim \mathcal{N}(\mathbf{0}, \Sigma)$, independent, identically distributed, and an estimate for $\Theta = \Sigma^{-1}$ is desired. The regularized likelihood function is maximized, leading to the optimization,

$$\hat{\Theta} = \underset{\Theta}{\operatorname{argmin}} \operatorname{tr}(S\Theta) - \log |\Theta| + \lambda \|\Theta\|_1 \quad (2)$$

where $S = \frac{1}{K}\mathbf{X}\mathbf{X}^T$ is the sample covariance matrix and $\|\Theta\|_1 = \sum_{i,j} |\Theta_{ij}|$.

For independent observations, the inverse covariance matrix corresponds to instantaneous second-order relations that can be useful for inference using graphical models. However, given time series data generated from a sparse graph process, the inverse covariance matrix Θ can actually reflect higher order effects and be significantly less sparse than the graph underlying the process. For example, if a process is described

by the dynamic equation with sparse state evolution matrix \mathbf{A} and $\|\mathbf{A}\|_2 \leq 1$,

$$\mathbf{x}[k] = \mathbf{A}\mathbf{x}[k-1] + \mathbf{w}[k]$$

where $\mathbf{w}[i]$ is a random noise process that is generated independently from $\mathbf{w}[j]$ for all $i \neq j$, then

$$\begin{aligned} \Sigma &= \mathbb{E} [\mathbf{x}[k]\mathbf{x}[k]^T] = \sum_{i=0}^{\infty} \mathbf{A}^i \mathbf{R} (\mathbf{A}^T)^i \\ \Rightarrow \Theta &= \left(\sum_{i=0}^{\infty} \mathbf{A}^i \mathbf{R} (\mathbf{A}^T)^i \right)^{-1} \end{aligned}$$

Even though the process can be described by sparse matrix \mathbf{A} , the true value of Θ represents powers of \mathbf{A} and need not be as sparse as \mathbf{A} . In addition, \mathbf{A} may not be symmetric, i.e. the underlying graph may be directed, while Θ is symmetric and the corresponding graph is undirected.

B. Sparse Vector Autoregressive Estimation

For time series data, instead of estimating the inverse covariance structure, sparse vector autoregressive (SVAR) estimation [14], [15], [9] recovers matrix coefficients for multivariate processes. This SVAR model assumes the time series at each node are conditionally independent from each other according to a Markov Random Field (MRF) with adjacency structure given by $\mathbf{A}' \in \{0, 1\}^{N \times N}$. This adjacency matrix \mathbf{A}' is closely related to Granger causality [16], [17] as shown in [9]. This problem assumes given data matrix of the form in equation (1) that is generated by the dynamic equation with sparse evolution matrices $\{\mathbf{A}^{(i)}\}$,

$$\mathbf{x}[k] = \sum_{i=1}^M \mathbf{A}^{(i)} \mathbf{x}[k-i] + \mathbf{w}[k]$$

where $\mathbf{w}[i]$ is a random noise process that is generated independently from $\mathbf{w}[j]$ for all times $i \neq j$, and $\mathbf{A}^{(i)}$ all have the same sparse structure. That is, $\mathbf{A}'_{ij} = 0 \Rightarrow \mathbf{A}^{(k)}_{ij} = 0$ for all k . Then SVAR solves the optimization,

$$\begin{aligned} \{\hat{\mathbf{A}}^{(i)}\} &= \underset{\{\mathbf{A}^{(i)}\}}{\operatorname{argmin}} \frac{1}{2} \sum_{k=M}^{K-1} \left\| \mathbf{x}[k] - \sum_{i=1}^M \mathbf{A}^{(i)} \mathbf{x}[k-i] \right\|_2^2 \\ &\quad + \lambda \sum_{i,j} \|\mathbf{a}_{ij}\|_2 \end{aligned} \quad (3)$$

where $\mathbf{a}_{ij} = \left(A_{ij}^{(1)} \quad \dots \quad A_{ij}^{(M)} \right)^T$ and the term $\|\mathbf{a}_{ij}\|_2$ promotes sparsity of the (i, j) -th entry of each $\mathbf{A}^{(i)}$ matrix simultaneously and thus also sparsity of \mathbf{A}' . This optimization can be solved using Group Lasso [12]. SVAR estimation methods estimate multiple weighted graphs $\mathbf{A}^{(i)}$ that can be used to estimate the sparsity structure \mathbf{A}' .

In contrast, our model is defined by a single weighted graph \mathbf{A} , but the corresponding time filter coefficients (introduced in section IV-A) are modeled as graph filters. In addition, using this single adjacency matrix \mathbf{A} and graph filters to describe the process enables principled analysis using the toolbox provided by the DSP_G framework.

C. Graph Signal Processing using the Laplacian

Frameworks for signal processing on graphs using the weighted (and/or possibly normalized) Laplacian matrix rather than the weighted adjacency matrix have been proposed [18], [19], [20]. For example, with a known graph Laplacian matrix, the polynomial coefficients for optimal graph filters can be learned and used to describe and compress signals [21]. The graph Laplacian also has the nice property that it is positive semidefinite, and so it has all real eigenvalues as well as a real orthonormal eigenvector matrix.

However, the Laplacian, which is symmetric, corresponding to an undirected graph, and can only have nonnegative real eigenvalues, is a restrictive representation for the dynamics of time series data through a graph. In contrast, the directed adjacency matrix may have negative as well as positive weights on edges and can have complex eigenvalues. Thus we choose to adopt the adjacency matrix as the basic building block for our model.

IV. GRAPH PROCESSES

Section IV-A presents our model for graph processes and section IV-B relates the approach to graph signal processing frameworks.

A. Causal Graph Process

Consider $x_n[k]$, a discrete time series on node v_n in graph $G = (\mathbf{V}, \mathbf{A})$, where n indexes the nodes of the graph and k indexes the time samples. Let N be the total number of nodes and K be the total number of time samples, and

$$\mathbf{x}[k] = (x_0[k] \ x_1[k] \ \dots \ x_{N-1}[k])^T \in \mathbb{C}^N$$

represents the graph signal at time sample k .

We consider a Causal Graph Process (CGP) to be a discrete time series $\mathbf{x}[k]$ on a graph $G = (\mathbf{V}, \mathbf{A})$ of the following form,

$$\begin{aligned} \mathbf{x}[k] &= \mathbf{w}[k] + \sum_{i=1}^M P_i(\mathbf{A}, \mathbf{c}) \mathbf{x}[k-i] \\ &= \mathbf{w}[k] + \sum_{i=1}^M \left(\sum_{j=0}^i c_{ij} \mathbf{A}^j \right) \mathbf{x}[k-i] \\ &= \mathbf{w}[k] + (c_{10} \mathbf{I} + c_{11} \mathbf{A}) \mathbf{x}[k-1] \\ &\quad + (c_{20} \mathbf{I} + c_{21} \mathbf{A} + c_{22} \mathbf{A}^2) \mathbf{x}[k-2] + \dots \\ &\quad + (c_{M0} \mathbf{I} + \dots + c_{MM} \mathbf{A}^M) \mathbf{x}[k-M] \end{aligned} \quad (4)$$

where $P_i(\mathbf{A}, \mathbf{c})$ is a matrix polynomial in \mathbf{A} , $\mathbf{w}[k]$ is statistical noise, c_{ij} are scalar polynomial coefficients, and

$$\mathbf{c} = (c_{10} \ c_{11} \ \dots \ c_{ij} \ \dots \ c_{MM})^T$$

is a vector collecting all the c_{ij} 's.

Note that the CGP model does *not* assume Markovianity on nodes and their neighbors imposed directly by the graph structure. It instead asserts that the signal on a node at the current time is affected through network effects by signals on other nodes at past times. Matrix polynomial $P_i(\mathbf{A}, \mathbf{c})$ is at most of order $\min(i, N_{\mathbf{A}})$, reflecting that $\mathbf{x}[k]$ cannot be influenced by more than i -th order network effects from i time

steps ago and in addition is limited (mathematically) by $N_{\mathbf{A}}$, the degree of the minimum polynomial of \mathbf{A} . Typically, we take the model order $M \ll N_{\mathbf{A}}$, and for the remainder of the paper assume this holds for sake of notational clarity.

This model captures the intuition that activity on the network travels at some fixed speed (one graph shift per sampling period), and thus the activity at the current time instant at a given network node cannot be affected by network effects of higher order than that speed allows. In this way, the CGP model can be seen as generalizing the spatial dimension of the light cone [22] to be on a discrete manifold rather than only on a lattice corresponding to uniformly sampled space.

The current parameterization of the CGP model given in (4) raises issues with identifiability. To address these issues, we assume that $P_1(\mathbf{A}, \mathbf{c}) \neq \alpha \mathbf{I}$ for any $\alpha \in \mathbb{R}$. Then, without further loss of generality, we can assume $c_{10} = 0$ and $c_{11} = 1$ so that $P_1(\mathbf{A}, \mathbf{c}) = \mathbf{A}$.

To verify this, consider the full parameterization using $(\mathbf{A}', \mathbf{c}')$. We show that we can instead use the reduced parameterization (\mathbf{A}, \mathbf{c}) with $P_1(\mathbf{A}, \mathbf{c}) = \mathbf{A}$ to represent the same process. First, we start with

$$\begin{aligned} P_1(\mathbf{A}', \mathbf{c}') &= c'_{10} \mathbf{I} + c'_{11} \mathbf{A}' = \mathbf{A} = P_1(\mathbf{A}, \mathbf{c}) \\ \Rightarrow \mathbf{A}' &= (c'_{11})^{-1} (\mathbf{A} - c'_{10} \mathbf{I}) \end{aligned} \quad (5)$$

We can invert c'_{11} , since by assumption $c'_{11} \neq 0$. Then consider the i -th polynomial,

$$\begin{aligned} P_i(\mathbf{A}', \mathbf{c}') &= \sum_{j=0}^i c'_{ij} (\mathbf{A}')^j = \sum_{j=0}^i c'_{ij} (c'_{11})^{-j} (\mathbf{A} - c'_{10} \mathbf{I})^j \\ &= \sum_{j=0}^i c'_{ij} (c'_{11})^{-j} \sum_{k=0}^j \binom{j}{k} (-c'_{10})^{j-k} \mathbf{A}^k \\ &= \sum_{k=0}^i \sum_{j=k}^i c'_{ij} (c'_{11})^{-j} \binom{j}{k} (-c'_{10})^{j-k} \mathbf{A}^k \\ &= \sum_{k=0}^i c_{ik} \mathbf{A}^k = P_i(\mathbf{A}, \mathbf{c}) \end{aligned} \quad (6)$$

when we define

$$c_{ik} = \sum_{j=k}^i c'_{ij} (c'_{11})^{-j} \binom{j}{k} (-c'_{10})^{j-k}$$

In the remainder of this paper, we assume that $P_1(\mathbf{A}, \mathbf{c}) \neq \alpha \mathbf{I}$ and use the reduced parameterization to ensure that \mathbf{A} and \mathbf{c} are uniquely specified without ambiguity.

B. Graph Signal Processing for Big Data

The $P_i(\mathbf{A}, \mathbf{c})$ from equation (4) can be seen in the DSP_G framework as causal graph filters. This allows us to naturally fit this model into the graph signal processing for big data framework, in which true graphs for large datasets can be expressed or approximated by graph products, which are sums of products, for example Kronecker products [23],

$$\mathbf{A}_0 = \sum_{i=1}^M \mathbf{A}_{ti} \otimes \mathbf{A}_{si}$$

in which \mathbf{A}_{ti} are jointly diagonalized by one eigenvector basis and \mathbf{A}_{si} are jointly diagonalized by a second eigenvector basis,

$$\begin{aligned}\mathbf{A}_{ti} &= \mathbf{V}_t \boldsymbol{\Lambda}_{ti} \mathbf{V}_t^{-1} \\ \mathbf{A}_{si} &= \mathbf{V}_s \boldsymbol{\Lambda}_{si} \mathbf{V}_s^{-1}\end{aligned}$$

This allows the eigen decomposition of \mathbf{A} to be found in terms of simpler decompositions of smaller matrices \mathbf{A}_{si} and \mathbf{A}_{ti} ,

$$\mathbf{A}_0 = \mathbf{V} \boldsymbol{\Lambda} \mathbf{V}^{-1} = \sum_{i=1}^M (\mathbf{V}_t \otimes \mathbf{V}_s) (\boldsymbol{\Lambda}_{ti} \otimes \boldsymbol{\Lambda}_{si}) (\mathbf{V}_t^{-1} \otimes \mathbf{V}_s^{-1})$$

For discrete time-series, the form of the time graph adjacency matrices is powers of the cyclic shift matrix $\mathbf{A}_{ti} = (\mathbf{C}^i)^T$, where

$$\mathbf{C} = \begin{pmatrix} & & & 1 \\ & & & \\ & & \ddots & \\ 1 & & & \end{pmatrix},$$

(only nonzero elements shown) representing the directed cycle graph and $\mathbf{A}_{si} = P_i(\mathbf{A})$. The diagonalizing matrix for the \mathbf{A}_{ti} is the Discrete Fourier Transform (DFT) matrix.

If this cyclic temporal structure is used to represent (4), we arrive at

$$\begin{aligned}\mathbf{X} &= \sum_{i=1}^M P_i(\mathbf{A}, \mathbf{c}) \mathbf{X} \mathbf{C}^i + \mathbf{W} \\ \Rightarrow \text{vec}(\mathbf{X}) &= \sum_{i=1}^M ((\mathbf{C}^i)^T \otimes P_i(\mathbf{A}, \mathbf{c})) \text{vec}(\mathbf{X}) + \text{vec}(\mathbf{W}) \\ &= \mathbf{A}_0 \text{vec}(\mathbf{X}) + \text{vec}(\mathbf{W})\end{aligned}\quad (7)$$

where \mathbf{X} is the data matrix defined as in (1) and \mathbf{W} is an error matrix. This corresponds to a wrapping around in time, which is not present in the model (4). While both forms of the model can be used to describe timeseries data, for the remainder of this paper, we will choose (4) to represent and estimate $P_i(\mathbf{A})$ from observed time series data.

V. ESTIMATING ADJACENCY MATRICES

Given a time series $\mathbf{x}(t)$ on graph $G = (\mathbf{V}, \mathbf{A})$ with *unknown* \mathbf{A} , we wish to estimate the adjacency matrix \mathbf{A} . A first approach to its estimation can be formulated as the following optimization problem,

$$\begin{aligned}(\mathbf{A}, \mathbf{c}) &= \underset{\mathbf{A}, \mathbf{c}}{\text{argmin}} \frac{1}{2} \sum_{k=M}^{K-1} \left\| \mathbf{x}[k] - \sum_{i=1}^M P_i(\mathbf{A}, \mathbf{c}) \mathbf{x}[k-i] \right\|_2^2 \\ &\quad + \lambda_1 \|\text{vec}(\mathbf{A})\|_1 + \lambda_2 \|\mathbf{c}\|_1\end{aligned}\quad (8)$$

where $\text{vec}(\mathbf{A})$ stacks the columns of the matrix \mathbf{A} .

In equation (8), the first term in the right hand side models $\mathbf{x}[k]$ by the CGP model in section IV-A, the regularizing term $\lambda_1 \|\text{vec}(\mathbf{A})\|_1$ promotes sparsity of the estimated adjacency matrix, and the term $\lambda_2 \|\mathbf{c}\|_1$ also promotes sparsity in the matrix polynomial coefficients. Regularizing \mathbf{c} corresponds to performing autoregressive model order selection. If the true model has $P_i(\mathbf{A}, \mathbf{c}) = \mathbf{0} \forall j \leq i \leq M$ for some $0 < j < M$, then regularization of \mathbf{c} encourages the corresponding values to be $\mathbf{0}$. The matrix polynomial in the first term makes this problem nonconvex. That is, using a convex optimization based approach to solve (8) directly may result in finding a

solution $(\hat{\mathbf{A}}, \hat{\mathbf{c}})$, minimizing the objective function locally, that is not near to the true globally minimizing (\mathbf{A}, \mathbf{c}) .

Instead, we break this estimation down into three separate, more tractable steps:

- 1) Solve for $\mathbf{R}_i = P_i(\mathbf{A}, \mathbf{c})$
- 2) Recover the structure of \mathbf{A}
- 3) Estimate c_{ij}

A. Solving for $P_i(\mathbf{A}, \mathbf{c})$

As previously stated, the graph filters $P_i(\mathbf{A}, \mathbf{c})$ are polynomials of \mathbf{A} and are thus shift-invariant and must mutually commute. Then their commutator

$$\begin{aligned}[P_i(\mathbf{A}, \mathbf{c}), P_j(\mathbf{A}, \mathbf{c})] &= \\ P_i(\mathbf{A}, \mathbf{c}) P_j(\mathbf{A}, \mathbf{c}) - P_j(\mathbf{A}, \mathbf{c}) P_i(\mathbf{A}, \mathbf{c}) &= 0 \quad \forall i, j\end{aligned}$$

Let $\mathbf{R} = (\mathbf{R}_1, \dots, \mathbf{R}_M)$; $\hat{\mathbf{R}}_i$ is the estimate of $P_i(\mathbf{A}, \mathbf{c})$. This leads to the optimization problem,

$$\begin{aligned}\hat{\mathbf{R}} &= \underset{\mathbf{R}}{\text{argmin}} \frac{1}{2} \sum_{k=M}^{K-1} \left\| \mathbf{x}[k] - \sum_{i=1}^M \mathbf{R}_i \mathbf{x}[k-i] \right\|_2^2 \\ &\quad + \lambda_1 \|\text{vec}(\mathbf{R}_1)\|_1 + \lambda_2 \sum_{i \neq j} \|\mathbf{R}_i, \mathbf{R}_j\|_F^2\end{aligned}\quad (9)$$

While this is still a non-convex problem, it is multi-convex. That is, when $\mathbf{R}_{-i} = \{\mathbf{R}_j : j \neq i\}$ (all \mathbf{R}_j except for \mathbf{R}_i) are held constant, the optimization is convex in \mathbf{R}_i . This naturally leads to block coordinate descent as a solution,

$$\begin{aligned}\hat{\mathbf{R}}_i &= \underset{\mathbf{R}_i}{\text{argmin}} \frac{1}{2} \sum_{k=M}^{K-1} \left\| \mathbf{x}[k] - \sum_{i=1}^M \mathbf{R}_i \mathbf{x}[k-i] \right\|_2^2 \\ &\quad + \lambda_1 \|\text{vec}(\mathbf{R}_1)\|_1 + \lambda_2 \sum_{j \neq i} \|\mathbf{R}_i, \mathbf{R}_j\|_F^2\end{aligned}\quad (10)$$

Each of these sub-problems for estimating \mathbf{R}_i in a single sweep of estimating \mathbf{R} is formulated as an ℓ_1 -regularized least-squares problem that can be solved using standard methods [24]. This has total complexity $O(MN^2K)$ incurred from minimizing over M separate blocks. The cost of the i -th problem is dominated in each iteration by $K - M$ matrix-vector products $\mathbf{R}_i \mathbf{x}[k-i]$ with total complexity $O(N^2(K-M))$ and by matrix-matrix products $\mathbf{R}_i \mathbf{R}_j$ for $j \neq i$ with complexity $O(MN^2)$.

B. Recovering \mathbf{A}

After obtaining estimates $\hat{\mathbf{R}}_i$, we find an estimate for \mathbf{A} . One approach is to take $\hat{\mathbf{A}} = \hat{\mathbf{R}}_1$. This appears to ignore the information from the remaining $\hat{\mathbf{R}}_i$. However, the information has already been incorporated during the iterations when solving for $\hat{\mathbf{R}}$, especially if we begin one new sweep to estimate \mathbf{R}_1 using (10) with $i = 1$. A second approach is also possible, explicitly using all the $\hat{\mathbf{R}}_i$ together to find \mathbf{A} ,

$$\begin{aligned}\hat{\mathbf{A}} &= \underset{\mathbf{A}}{\text{argmin}} \left\| \hat{\mathbf{R}}_1 - \mathbf{A} \right\|_2^2 + \lambda_1 \|\text{vec}(\mathbf{A})\|_1 \\ &\quad + \lambda_2 \sum_{i=2}^M \left\| \mathbf{A}, \hat{\mathbf{R}}_i \right\|_F^2\end{aligned}\quad (11)$$

This can be seen as similar to running one additional step further in the block coordinate descent to find $\widehat{\mathbf{R}}_1$ except that this approach does not explicitly use the data. This has complexity $O(MN^2)$ dominated by matrix-matrix products $A\mathbf{R}_i$ for $i \neq 1$.

C. Estimating \mathbf{c}

We can estimate c_{ij} in one of two ways: we can estimate \mathbf{c} either from $\widehat{\mathbf{A}}$ and $\widehat{\mathbf{R}}_i$ or from $\widehat{\mathbf{A}}$ and the data \mathbf{X} .

To estimate c_{ij} from $\widehat{\mathbf{A}}$ and $\widehat{\mathbf{R}}_i$, we set up the optimization,

$$\widehat{\mathbf{c}}_i = \underset{\mathbf{c}_i}{\operatorname{argmin}} \frac{1}{2} \left\| \widehat{\mathbf{R}}_i - \mathbf{Q}_i \mathbf{c}_i \right\|_2^2 + \lambda_3 \|\mathbf{c}_i\|_1 \quad (12)$$

where

$$\mathbf{Q}_i = \begin{pmatrix} \operatorname{vec}(\mathbf{I}) & \operatorname{vec}(\widehat{\mathbf{A}}) & \dots & \operatorname{vec}(\widehat{\mathbf{A}}^i) \end{pmatrix},$$

$$\mathbf{c}_i = (c_{i0} \quad c_{i1} \quad \dots \quad c_{ii})^T$$

Alternatively, to estimate c_{ij} from $\widehat{\mathbf{A}}$ and the data \mathbf{X} , we can use the optimization,

$$\widehat{\mathbf{c}} = \underset{\mathbf{c}}{\operatorname{argmin}} \frac{1}{2} \|\mathbf{Y} - \mathbf{B}\mathbf{c}\|_F^2 + \lambda_3 \|\mathbf{c}\|_1 \quad (13)$$

where $\mathbf{Y} = \operatorname{vec}(\mathbf{X}_M)$,

$$\mathbf{B} = \left(\operatorname{vec}(\mathbf{X}_{M-1}) \dots \operatorname{vec}(\widehat{\mathbf{A}}^i \mathbf{X}_{M-j}) \dots \operatorname{vec}(\widehat{\mathbf{A}}^M \mathbf{X}_0) \right),$$

$$\mathbf{X}_m = \begin{pmatrix} \mathbf{x}[m] & \mathbf{x}[m+1] & \dots & \mathbf{x}[m+K-M-1] \end{pmatrix},$$

which can also be solved using standard ℓ_1 -regularized least squares methods with complexity $O(M^2N(K-M))$, dominated by computing matrix-vector products with \mathbf{B} and \mathbf{B}^\top .

D. General Estimation

The methods discussed so far can be interpreted as assuming that 1) the process is a linear autoregressive process driven by white Gaussian noise and 2) the elements in parameters \mathbf{A} and \mathbf{c} a priori follow zero-mean Laplace distributions. The objective function in (8) approximately corresponds to the log posterior density and its solution to an approximate maximum a posteriori (MAP) estimate.

This framework can be extended to estimate more general autoregressive processes, such as those with a non-Gaussian noise model and certain forms of nonlinear dependence of the current state on past values of the state. We formulate the general optimization

$$\begin{aligned} (\widehat{\mathbf{A}}, \widehat{\mathbf{c}}) = \underset{\mathbf{A}, \mathbf{c}}{\operatorname{argmin}} & f(\mathbf{X}, P_1(\mathbf{A}, \mathbf{c}), \dots, P_M(\mathbf{A}, \mathbf{c})) \\ & + g_1(\mathbf{A}) + g_2(\mathbf{c}) \end{aligned} \quad (14)$$

where $f(\cdot, \dots, \cdot)$ is a loss function that corresponds to a log-likelihood function dictated by the noise model, and $g_1(\cdot)$ and $g_2(\cdot)$ are regularization functions (usually convex norms) that correspond to log-prior distributions imposed on the parameters and are dictated by modeling assumptions. Again, the matrix polynomials $P_i(\mathbf{A}, \mathbf{c})$ introduce nonconvexity, so similarly as before, we can separate the estimation into three steps to reduce complexity.

We next generalize equation (10) used to find \mathbf{R}_i as estimates of $P_i(\mathbf{A}, \mathbf{c})$ with the optimization

$$\begin{aligned} \widehat{\mathbf{R}}_i = \underset{\mathbf{R}_i}{\operatorname{argmin}} & f_i(\mathbf{X}, \mathbf{R}_i) + g_{1i}(\mathbf{R}_i) \\ & + g_{2i}([\mathbf{R}_i, \widehat{\mathbf{R}}_1], \dots, [\mathbf{R}_i, \widehat{\mathbf{R}}_M]) \end{aligned} \quad (15)$$

where $f_i(\cdot, \cdot)$ is the part of the objective function that depends on $P_i(\mathbf{A}, \mathbf{c})$ when the other \mathbf{R}_{-i} are fixed, the term $g_{1i}(\cdot)$ regularizes the estimated matrix polynomial, and the term $g_{2i}(\cdot, \dots, \cdot)$ promotes commutativity of the matrix polynomials.

Next, we can again take $\mathbf{A} = \mathbf{R}_1$, or we can reformulate equation (11)

$$\widehat{\mathbf{A}} = \underset{\mathbf{A}}{\operatorname{argmin}} f(\widehat{\mathbf{R}}_1, \mathbf{A}) + g_1(\mathbf{A}) + g_2(\mathbf{A}, \widehat{\mathbf{R}}_{-1}) \quad (16)$$

where $f(\cdot)$ is a loss function, $g_1(\cdot)$ regularizes the estimated adjacency matrix, and $g_2(\mathbf{A}, \mathbf{R}_{-1})$ enforces commutativity of the adjacency matrix with the other matrix polynomials.

We generalize (12) as

$$\widehat{\mathbf{c}}_i = \underset{\mathbf{c}_i}{\operatorname{argmin}} f(\widehat{\mathbf{R}}_i, \mathbf{Q}_i \mathbf{c}_i) + g(\mathbf{c}_i) \quad (17)$$

where $f(\cdot)$ is the objective function, and $g(\cdot)$ is a regularizing function on the matrix polynomial coefficients, and \mathbf{Q}_i is defined as in section V-C; and lastly we generalize (13) as

$$\widehat{\mathbf{c}} = \underset{\mathbf{c}}{\operatorname{argmin}} f(\mathbf{Y}, \mathbf{B}\mathbf{c}) + g(\mathbf{c}) \quad (18)$$

where $f(\cdot)$ and $g(\cdot)$ are the same functions as above in (17), and \mathbf{Y} and \mathbf{B} are defined as in section V-C.

Algorithm 1 outlines this 3-step algorithm to obtain estimates $\widehat{\mathbf{A}}$ and $\widehat{\mathbf{c}}$ for the adjacency matrix and filter coefficients; it is a more efficient and well-behaved alternative to directly using (14).

Algorithm 1 Base estimation algorithm

```

Initialize,  $t = 0$ ,  $\widehat{\mathbf{R}}^{(t)} = \mathbf{0}$ 
while  $\widehat{\mathbf{R}}^{(t)}$  not converged do
  for  $i = 1 : M$  do
    Find  $\widehat{\mathbf{R}}_i^{(t)}$  with fixed  $\widehat{\mathbf{R}}_{<i}^{(t)}$ ,  $\widehat{\mathbf{R}}_{>i}^{(t-1)}$  using (15).
  end for
   $t \leftarrow t + 1$ 
end while
Set  $\widehat{\mathbf{A}} = \widehat{\mathbf{R}}_1^{(\tau)}$  or estimate  $\widehat{\mathbf{A}}$  from  $\widehat{\mathbf{R}}^{(\tau)}$  using (16).
Solve for  $\widehat{\mathbf{c}}$  from  $\mathbf{X}$ ,  $\widehat{\mathbf{A}}$  using (17) or from  $\mathbf{X}$ ,  $\widehat{\mathbf{R}}$  using (18).

```

We call this 3-step procedure the base algorithm. In algorithm 1, superscripts denote the iteration number, $\widehat{\mathbf{R}}_{<i}^{(t)}$ denotes $\{\widehat{\mathbf{R}}_j^{(t)} : j < i\}$ and likewise $\widehat{\mathbf{R}}_{>i}^{(t)}$ denotes $\{\widehat{\mathbf{R}}_j^{(t)} : j > i\}$, and τ is the final iteration performed before convergence of $\widehat{\mathbf{R}}$ is determined or a preset maximum iteration count is exceeded.

E. Simplified Estimation

The base algorithm can still be moderately expensive to evaluate computationally when scaling to larger problems and is difficult to analyze theoretically, mainly due to the nonconvexity of the commutativity-enforcing term. For further ease of computation and analysis, we consider a simplified version of the base algorithm in which the commutativity term of the optimization problem (10) is removed. We call this the Simplified Algorithm, described in algorithm 2.

$$\widehat{\mathbf{R}} = \underset{\mathbf{R}}{\operatorname{argmin}} f(\mathbf{X}, \mathbf{R}) + g(\mathbf{R}) \quad (19)$$

This can be followed by the same steps to find $\widehat{\mathbf{A}}$ and $\widehat{\mathbf{c}}$ as in the base algorithm, taking $\widehat{\mathbf{A}} = \widehat{\mathbf{R}}_1$ or as the solution to (11), and then solving (17) or (18) for $\widehat{\mathbf{c}}$. Using standard solvers for the estimation in (19) with ℓ_2 and ℓ_1 norms as seen before, the cost is $O(MN^2(K - M))$, dominated by computing the matrix-vector product $\mathbf{R}_i \mathbf{x}[k - i]$ for $i = 1, \dots, M$ and for $k = M, \dots, K$.

Algorithm 2 Simplified estimation algorithm

Initialize $\widehat{\mathbf{R}} = \mathbf{0}$
 Estimate $\widehat{\mathbf{R}}$ using (19)
 Set $\widehat{\mathbf{A}} = \widehat{\mathbf{R}}_1$ or estimate $\widehat{\mathbf{A}}$ from $\widehat{\mathbf{R}}$ using (16).
 Solve for $\widehat{\mathbf{c}}$ from \mathbf{X} , $\widehat{\mathbf{A}}$ using (17) or from \mathbf{X} , $\widehat{\mathbf{R}}$ using (18).

F. Extension of Estimation

As an extension of the base algorithm, we can also choose the estimated matrix $\widehat{\mathbf{A}}$ and filter coefficients $\widehat{\mathbf{c}}$ to initialize the direct approach of using (14). Starting from these initial estimates, we may find better local minima than with initializations at $\mathbf{A} = \mathbf{0}$ and $\mathbf{c} = \mathbf{0}$ or at random estimates. We call this procedure the extended algorithm, summarized in algorithm 3.

Algorithm 3 Extended estimation algorithm

Estimate $\mathbf{A}^{(0)}$, $\mathbf{c}^{(0)}$ using basic algorithm.
 Find $\widehat{\mathbf{A}}$, $\widehat{\mathbf{c}}$ using initialization $\mathbf{A}^{(0)}$, $\mathbf{c}^{(0)}$ from (14) using convex methods.

VI. CONVERGENCE OF ESTIMATION

In this section, we discuss the convergence of the basic, extended, and simplified algorithms described above.

A. Base Algorithm

In estimating \mathbf{A} and \mathbf{c} , the forms of the optimization problems are well studied when choosing ℓ_2 and ℓ_1 norms as loss and regularization functions, as seen in equations (11) and (13). However, using these same norms, step 1 of the algorithm is a nonconvex optimization. Hence we would like to ensure that step 1 converges.

When using block coordinate descent (i.e., repeatedly choosing one block of coordinate directions in which to optimize while holding all other blocks constant) for general functions, neither the solution nor the objective function values are guaranteed to converge to a global or even a local minimum. However, under some mild assumptions, using block coordinate descent to estimate \mathbf{R}_i will converge. In equation (14), if we assume the objective function to be continuous and to have convex, compact sublevel sets in each coordinate block \mathbf{R}_i (for example, if the functions for f and g are the ℓ_2 and ℓ_1 norms as in equation (8)), then the block coordinate descent will converge [25].

B. Extended Algorithm

Now we discuss the convergence of the extended method described in section V-F assuming that the basic algorithm has converged to an initial point $(\mathbf{A}^{(0)}, \mathbf{c}^{(0)})$ for the extended algorithm. We assume that the function $F = f + g_1 + g_2$ in equation (14) has compact sublevel sets and is bounded below. Then an iterative gradient or Newton method with appropriately chosen step sizes that produces updates of $(\mathbf{A}^{(t+1)}, \mathbf{c}^{(t+1)})$ such that $F(\mathbf{A}^{(t+1)}, \mathbf{c}^{(t+1)}) \leq F(\mathbf{A}^{(t)}, \mathbf{c}^{(t)})$ converges, possibly to a local optimum if the problem is nonconvex [26]. If the functions are the ℓ_2 and ℓ_1 norms as in equation (8), these conditions are satisfied as well.

C. Simplified Algorithm

Here we outline the theoretical performance guarantees of the simplified estimate $(\widehat{\mathbf{A}}, \widehat{\mathbf{c}})$ when using ℓ_1 regularized least squares to estimate $\widehat{\mathbf{R}}$,

$$\widehat{\mathbf{R}} = \underset{\mathbf{R}}{\operatorname{argmin}} \sum_{k=M}^{K-1} \|\mathbf{x}[k] - \sum_{i=1}^M \mathbf{R}_i \mathbf{x}[k - i]\| + \lambda_1 \|\operatorname{vec}(\mathbf{R})\|_1 \quad (20)$$

which is a special case of (19), and then using $\widehat{\mathbf{A}} = \widehat{\mathbf{R}}_1$ and the optimization (13) to find $\widehat{\mathbf{c}}$.

Our error metric of interest will be:

$$\epsilon = \mathbb{E} \left[\frac{1}{N} \left\| \mathbf{x}[k] - f(\widehat{\mathbf{A}}, \widehat{\mathbf{c}}, \mathbf{X}_{k-1}) \right\|_2^2 \right] - \mathbb{E} \left[\frac{1}{N} \left\| \mathbf{x}[k] - f(\mathbf{A}, \mathbf{c}, \mathbf{X}_{k-1}) \right\|_2^2 \right] \quad (21)$$

where

$$\mathbf{X}_{k-1} = \begin{pmatrix} \mathbf{x}[k-1] & \mathbf{x}[k-2] & \dots & \mathbf{x}[k-M] \end{pmatrix}$$

and $f(\mathbf{A}, \mathbf{c}, \mathbf{X}_{k-1}) = \sum_{i=1}^M P_i(\mathbf{A}, \mathbf{c}) \mathbf{x}[k - i]$. This error ϵ is the average excess prediction risk. This quantity is the per-node error above the intrinsic randomness of the true CGP that the prediction of the next observation that the estimated CGP exhibits. The expectation is taken over a new sample

$$\mathbf{z}_k = \left(\mathbf{x}[k]^\top \mathbf{X}_{k-1}^\top \right)^\top \quad (22)$$

drawn independently of the samples used to estimate $(\widehat{\mathbf{A}}, \widehat{\mathbf{c}})$.

1) *Assumptions:* First, we list the assumptions we make about the true process in order to derive our guarantees:

- (A1) The CGP model class is accurate:
 $\mathbb{E}[\mathbf{x}[k] | \mathbf{X}_{k-1}] = f(\mathbf{A}, \mathbf{c}, \mathbf{X}_{k-1})$.
- (A2) The noise process is uncorrelated with the CGP and its own past values:
 $\mathbb{E}[\mathbf{x}[j] \mathbf{w}[k]^\top] = \mathbf{0}$ and $\mathbb{E}[\mathbf{w}[j] \mathbf{w}[k]^\top] = \mathbf{0}$ for $j \leq k$.
 In particular, the noise is multivariate Gaussian with distribution $\mathbf{w}[k] \sim \mathcal{N}(\mathbf{0}, \Sigma_{\mathbf{w}})$, with $0 < \sigma_\ell \leq \|\Sigma_{\mathbf{w}}^{-1}\|^{-1}$ and $\|\Sigma_{\mathbf{w}}\| \leq \sigma_u$ (the smallest and largest singular values) being lower and upper bounded.
- (A3) The CGP is stationary and is already in steady state when we begin sampling. Under this assumption, the marginal distributions and expectations are, $\mathbb{E}[\mathbf{x}[k]] = \mathbf{0}$, $\Sigma_0 = \mathbb{E}[\mathbf{x}[k] \mathbf{x}[k]^\top]$, and $\Sigma = \mathbb{E}[\mathbf{z}_k \mathbf{z}_k^\top]$ where \mathbf{z}_k is defined as in (22).
- (A4) The stationary correlation matrices are absolutely summable:

$$\sum_{i=-\infty}^{\infty} \|\mathbb{E}[\mathbf{x}[k]\mathbf{x}[k-i]^\top]\| = G < \infty.$$

This is a slightly stronger condition than stationarity.

(A5) The true adjacency matrix and filter coefficients are sparse and bounded:

$$\begin{aligned} \left\| \begin{pmatrix} \mathbf{A} & P_2(\mathbf{A}, \mathbf{c}) & \dots & P_M(\mathbf{A}, \mathbf{c}) \end{pmatrix} \right\|_1 &\leq S_{MN} \ll MN^2 \\ \left\| \begin{pmatrix} \mathbf{A} & P_2(\mathbf{A}, \mathbf{c}) & \dots & P_M(\mathbf{A}, \mathbf{c}) \end{pmatrix} \right\|_0 &\leq s_{MN} \ll MN^2 \end{aligned}$$

and $\max_{1 \leq i \leq M} (\|P_i(\mathbf{A})\|) \leq L$; $\|\mathbf{c}\|_2 \leq \|\mathbf{c}\|_1 \leq \rho$. Also, $(1+L)(1+\rho) = Q \leq 2$. This is also a slightly stronger condition than stationarity. The quantities S_{MN} and s_{MN} with subscripts may grow with M and N .

(A6) The sample size is large enough relative to the ‘‘stability’’ of the process:

$$T = K - M \geq C\omega^2 s_N (\log M + \log N)$$

for some constant $C > 0$ and $\omega = \frac{\sigma_u}{\sigma_\ell} \frac{Q^2}{\mu_{\min}(\tilde{\mathbf{A}})}$. Here ω and $\mu_{\min}(\tilde{\mathbf{A}})$ are related to measures of ‘‘stability’’ of the process [27], and their explicit forms are given in the appendix A.

2) *Theoretical Performance:* Here, we present the main guarantee and a brief sketch for its proof, making note of several lemmas of intermediate results used in the main result. The full proof is presented in Appendices A-D.

Lemma 1. *Assume (A1) that $\mathbf{x}[k]$ is generated according to the CGP model with \mathbf{A} satisfying (A5). Suppose (A6) that the sample size K is large enough. Then there exist constants $d_i > 0$ such that, for $\lambda \geq 4g(Q)\sigma_u\sqrt{(\log M + \log N)/K}$, with probability at least $1 - d_1 \exp\{-d_2 K/\omega^2\}$, the solution to (20) satisfies the inequalities*

$$\begin{aligned} \|\tilde{\mathbf{A}} - \mathbf{A}\|_1 &\leq 64\lambda s_{MN} Q^2 / \sigma_\ell \\ \|\tilde{\mathbf{A}} - \mathbf{A}\|_2 &\leq \|\tilde{\mathbf{A}} - \mathbf{A}\|_F \leq 16\lambda\sqrt{s_{MN}} Q^2 / \sigma_\ell \end{aligned}$$

where ω is defined as in (A6) and $g(Q) = d_3 \left(1 + \frac{1+Q^2}{(2-Q)^2}\right)$.

Lemma 1 states that if the sample size K is large enough relative to network size N , sparsity s_{MN} , and other problem parameters, then with high probability the estimate $\tilde{\mathbf{A}}$ from (19) is not too different from the true \mathbf{A} . The statement of this lemma is adapted to this problem from the assumptions and Propositions 4.1-4.3 from [27].

The following lemma is a uniform concentration result on quadratic forms of Gaussian vectors.

Lemma 2. *Let $\mathbf{x} = (X_1, \dots, X_n) \sim \mathcal{N}(\mathbf{0}, \mathbf{I}_n)$ and let $\mathcal{B} = \{\mathbf{B} : \|\mathbf{B}\| \leq J\} \subset \mathbb{R}^{n \times n}$ for some $0 < J < \infty$ be a set of real matrices, not necessarily symmetric. Then, for $0 \leq t \leq Jn/3$,*

$$\begin{aligned} P\left(\sup_{\mathbf{B} \in \mathcal{B}} \left(\mathbf{x}^\top \mathbf{B} \mathbf{x} - \mathbb{E}[\mathbf{x}^\top \mathbf{B} \mathbf{x}]\right) > t\right) &\leq \delta \\ P\left(\sup_{\mathbf{B} \in \mathcal{B}} \left(\mathbb{E}[\mathbf{x}^\top \mathbf{B} \mathbf{x}] - \mathbf{x}^\top \mathbf{B} \mathbf{x}\right) > t\right) &\leq \delta \end{aligned}$$

where $\delta = \frac{1}{e} \left(\frac{2e}{n}\right)^{n/2} + \exp\left\{-\frac{27}{64} \frac{t^2}{J^2 n}\right\}$.

The next lemma follows from an application of Lemma 2 to this problem.

Lemma 3 (Based on Lemma 2). *Under assumptions (A1)-(A6), for any $0 \leq \beta \leq 1$, with probability at least $1 -$*

$2 \left(\frac{1}{e} \left(\frac{2e}{NK}\right)^{NK/2} + \exp\left\{-\frac{3}{64}(NK)^\beta\right\}\right)$, the following holds:

$$\begin{aligned} &\mathbb{E} \left[\frac{1}{N} \left\| \mathbf{x}[k] - f(\tilde{\mathbf{A}}, \tilde{\mathbf{c}}, \mathbf{X}_{k-1}) \right\|_2^2 \right] \\ &- \mathbb{E} \left[\frac{1}{N} \left\| \mathbf{x}[k] - f(\tilde{\mathbf{A}}, \mathbf{c}, \mathbf{X}_{k-1}) \right\|_2^2 \right] \\ &\leq \frac{1}{NT} \sum_{k=M}^{T-1} \left\| \mathbf{x}[k] - f(\tilde{\mathbf{A}}, \tilde{\mathbf{c}}, \mathbf{X}_{k-1}) \right\|_2^2 \\ &- \frac{1}{NT} \sum_{k=M}^{T-1} \left\| \mathbf{x}[k] - f(\tilde{\mathbf{A}}, \mathbf{c}, \mathbf{X}_{k-1}) \right\|_2^2 + \frac{2GQ^2K}{T(NK)^{(1-\beta)/2}} \end{aligned} \quad (23)$$

We are ready to present the main performance guarantee.

Theorem 4 (Main result). *Under Assumptions (A1)–(A6) and using the same notations, for some constants $d_i > 0$ and for all $0 \leq \beta \leq 1$, with probability at least*

$$1 - \left(\frac{2}{e} \left(\frac{2e}{NK}\right)^{\frac{NK}{2}} + 2 \exp\left(-\frac{3}{64}(NK)^\beta\right) + d_2 \exp\left(-\frac{d_3}{\omega^2} T\right) \right),$$

the error satisfies

$$\epsilon \leq d_1 \frac{L^2 \delta^2}{N} \left(\tilde{L}_M(\delta)\right)^2 \text{tr}(\Sigma_0) + \frac{2GQ^2K}{T(NK)^{(1-\beta)/2}} \quad (24)$$

where $\delta^2 = \frac{\log M + \log N}{T} \frac{\sigma_u^2}{\sigma_\ell^2} Q^4 (g(Q))^2 s_{MN}$ with

$$g(Q) = d_3 \left(1 + \frac{1+Q^2}{(2-Q)^2}\right) \text{ and } \tilde{L}_M(\delta) = \max_{1 \leq i \leq M} \frac{(L+\delta)^i - L^i}{\delta}$$

This theorem states that as the number of nodes N and the number of time observations K grow, with high probability, the average excess prediction risk of the simplified estimate is not too large. This holds if M grows slowly enough with respect to K and to N . Note that for large N and K , we have $\delta \ll L$, and the factor $\tilde{L}_M(\delta) = O(ML^{M-1})$. The full proof is in Appendix D, but we provide a brief overview here.

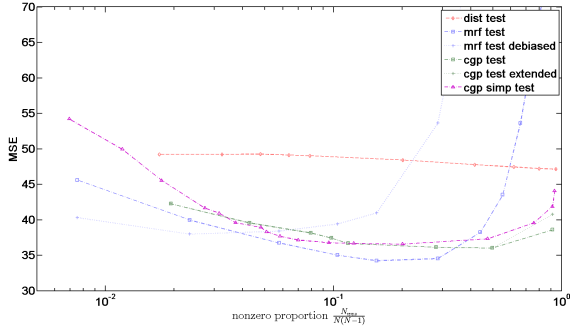
Proof Sketch. With similar algebra to [28], we can show that

$$\begin{aligned} \epsilon &= \frac{1}{N} \mathbb{E} \left[\left\| f(\tilde{\mathbf{A}}, \mathbf{c}, \mathbf{X}_{k-1}) - f(\mathbf{A}, \mathbf{c}, \mathbf{X}_{k-1}) \right\|_2^2 \right] \\ &+ \frac{1}{N} \left(\mathbb{E} \left[\left\| \mathbf{x}[k] - f(\tilde{\mathbf{A}}, \tilde{\mathbf{c}}, \mathbf{X}_{k-1}) \right\|_2^2 \right] - \left\| \mathbf{x}[k] - f(\tilde{\mathbf{A}}, \mathbf{c}, \mathbf{X}_{k-1}) \right\|_2^2 \right) \end{aligned}$$

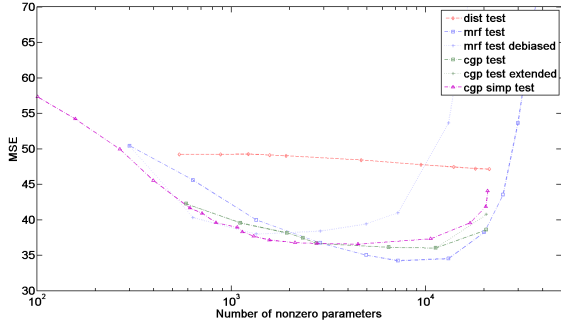
With considerable effort and several additional insights, we can bound these two terms. We bound the first term using the result from AR estimation in Lemma 1. With a bit of additional algebra and concentration results on Chi-squared distributions from Lemma 3, we can bound the second term (in parentheses) by its empirical version (plus small error) with high probability. Arguing that the empirical version is negative as a result of the optimization (13), we arrive at our result. \square

VII. EXPERIMENTS

We test our algorithms on two types of datasets, a real temperature sensor network timeseries (with $N = 150$ and $K = 365$) and a synthetically generated timeseries (with varying N and K). With the temperature dataset, we compare the performance of the CGP model against that of the sparse vector autoregressive Markov random field model (labeled



(a) Testing Errors vs Sparsity



(b) Testing Errors vs Nonzero Parameters

Fig. 1. Compression and Prediction Error vs Nonzeros using order $M = 2$ model

as MRF); with the synthetic dataset, we compare the model parameters and performance to the ground truth used to generate the data.

To solve the regularized least squares iterations for estimating the CGP matrices, we used a fast implementation of proximal quasi-Newton optimization for ℓ_1 regularized problems [29]. To estimate the MRF matrices, we used an accelerated proximal gradient descent algorithm [30] to estimate the SVAR matrix coefficients from equation (3) since the code used in [9] is not tested for larger graphs.

A. Temperature Data

The temperature dataset is a collection of daily average temperature measurements taken over 365 days at 150 locations around the continental United States [31]. The time series \mathbf{x}_i is detrended by a 4th order polynomial at each measurement station i to form $\tilde{\mathbf{x}}_i$. The data matrix \mathbf{X} is formed from stacking $\tilde{\mathbf{x}}_i$

We compare the prediction errors of using the CGP and MRF models as well as an undirected distance graph as described in [3], all on the same set of temperature data. The distance graph model uses an adjacency matrix \mathbf{A}^{dist} to model the process

$$\mathbf{x}[k] = \mathbf{w}[k] + \sum_{i=1}^M h_i(\mathbf{A}^{\text{dist}})\mathbf{x}[k-i]$$

where $h_i(\mathbf{A}^{\text{dist}}) = \sum_{j=0}^L c_{ji}(\mathbf{A}^{\text{dist}})^j$ are polynomials of the distance matrix with elements chosen as

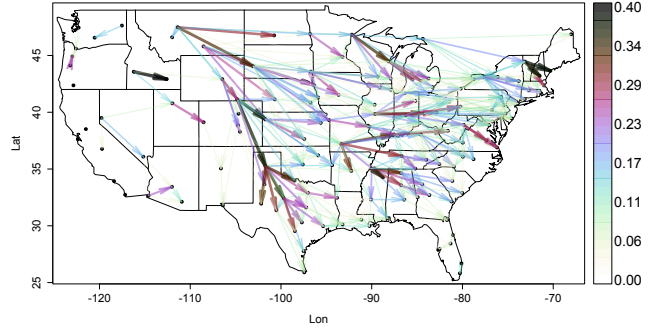


Fig. 2. Estimated CGP temperature graph using order $M = 2$ model with sparsity $p_{\text{nnz}} = 0.05$

$$\mathbf{A}_{mn}^{\text{dist}} = \frac{e^{-d_{mn}^2}}{\sqrt{\sum_{j \in \mathcal{N}_n^k} e^{-d_{nj}^2} \sum_{\ell \in \mathcal{N}_m^k} e^{-d_{m\ell}^2}}}$$

with \mathcal{N}_n^k representing the neighborhood of k cities nearest to city n and d_{mn} being the geographical distance between cities m and n . In this model, M is taken to be fixed and the polynomial coefficients c_{ji} are to be estimated. In our experiments, we assumed $M = 2$.

We separated the data into two segments, one consisting of the even time indices and one consisting of the odd time indices. One set was used as training data and the other set was left as testing data. This way, the test and training data were both generated from almost the same process but with different daily fluctuations. In this experiment, we compute the prediction MSE as

$$MSE = \frac{1}{N(K-M)} \sum_{i=M+1}^K \|\mathbf{x}[i] - \hat{\mathbf{x}}[i]\|^2$$

Here, since we do not have the ground truth graph for this data, the experiments can be seen as corresponding to the task of prediction. The test error indicates how well the estimated graph can predict the following time instance from past observations on new series, while the training error is not as indicative of actual performance for the prediction task. We used a grid of sparsity regularization parameters λ and used the λ corresponding to the lowest training error to estimate the model on test data and determine the test error.

Figure 1(a) shows the prediction performance of various algorithms as a function of edge sparsity of the respective graphs. We see that directed graphs estimated from data (either CGP or MRF) perform better in testing than undirected distance graphs derived independently of the data. In addition, for high sparsity or low nonzeros ($p_{\text{nnz}} = \frac{N_{\text{nnz}}}{N(N-1)} < 0.3$, where p_{nnz} is the proportion of nonzero edges in the graph and N_{nnz} is the number of nonzero edges in the graph, not including self-edges), the performance of the CGP is competitive with the MRF model. At lower sparsity levels ($p_{\text{nnz}} > 0.3$), the MRF model performs better than the CGP model in minimizing training error (not shown), but not in testing.

Figure 1(b) shows the prediction performance of various algorithms as a function of total nonzero parameters of the respective models. The same trends are present here as well. Here, for the CGP model, the number of nonzero parameters is calculated $N_{\text{param}}^{\text{CGP}} = N_{\text{nnz}}^{\text{CGP}} + N + M_{\text{nnz}}^{\text{CGP}}$, where N includes

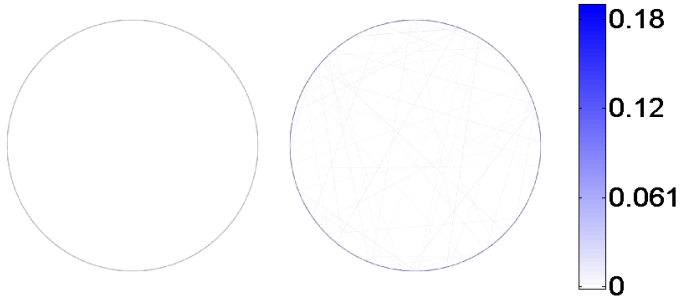
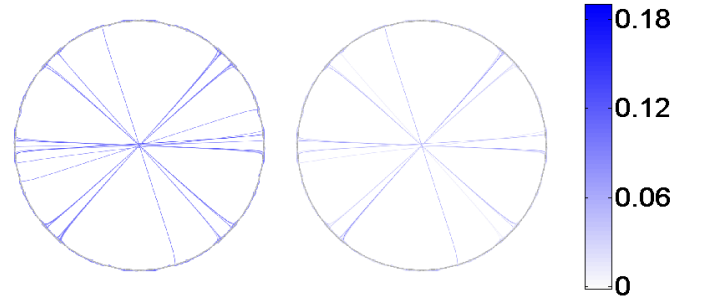
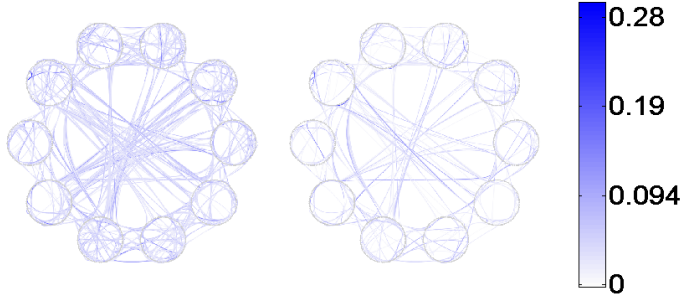
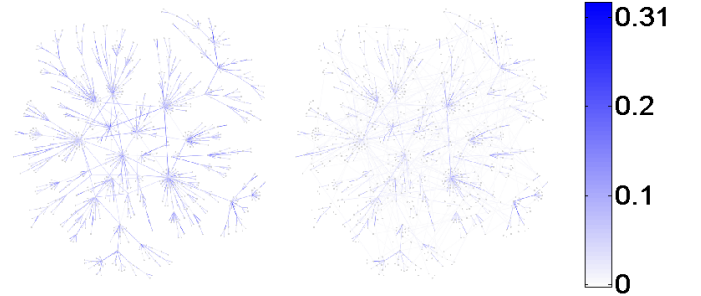
(a) True \mathbf{A} (left) and Estimated $\hat{\mathbf{A}}$ (right) for KR graph(a) True \mathbf{A} (left) and Estimated $\hat{\mathbf{A}}$ (right) for ER graph(b) True \mathbf{A} (left) and Estimated $\hat{\mathbf{A}}$ (right) for SBM graph(b) True \mathbf{A} (left) and Estimated $\hat{\mathbf{A}}$ (right) for PL graph

Fig. 3. True (left) and estimated (right) edge weights (absolute values) for KR (top row) and SBM (bottom row) graphs for $N=1000$

Fig. 4. True (left) and estimated (right) edge weights (absolute values) for ER (top row) and SBM (bottom row) graphs for $N=1000$

the diagonal and $M_{nnz}^{CGP} \leq M(M+1) - 3$ counts the nonzeros in \mathbf{c} . For the MRF model, the number of nonzero parameters is calculated $N_{\text{param}}^{MRF} = M(N_{nnz}^{MRF} + N)$, where N includes the diagonal and the factor of M accounts for the fact that the nonzero entries of $\mathbf{A}^{(i)}$ can be different across i . Here, the CGP has lower test error than MRF with fewer nonzero parameters ($N_{nnz} < 2000$).

In figure 2, we visualize the temperature network estimated on the entire time series using the CGP and model that has sparsity level $p_{nnz} = 0.05$. The x -axis corresponds to longitude while the y -axis corresponds to latitude. We see that the CGP model clearly picks out the predominant west-to-east direction of wind in the $x \geq -95$ portion of the country, as single points in this region are seen to predict multiple eastward points. It also shows the influence of the roughly north-northwest-to-south-southeast Rocky Mountain chain at $-110 \leq x \leq -100$. This CGP graph paints a picture of US weather patterns that is consistent with geographic and meteorological features.

B. Synthetic Data

We test our simplified algorithm on larger synthetic datasets to empirically verify the theory developed in section VI.

The random graphs corresponding to \mathbf{A} were generated with 4 different topologies: k -regular (KR), stochastic blockmodel (SBM) [32], Erdős-Renyi (ER) [33], and power law (PL).

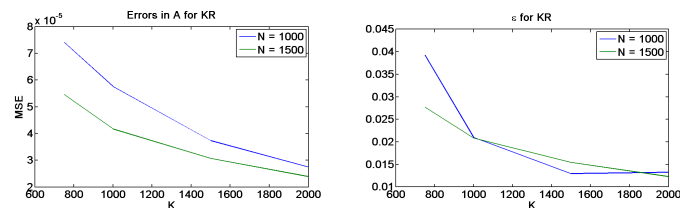
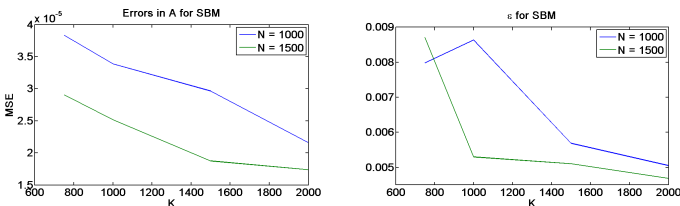
The KR graph was generated by taking a circle graph and connecting each node to itself using a weight of -1 and to its $k = 3$ neighbors to each side on the circle with weights drawn from a random uniform distribution $\mathcal{U}(0.5, 1)$. This resulted in a $(2k+1)$ -diagonal (in this case heptadiagonal) matrix. Finally the matrix was normalized by 1.5 times its largest eigenvalue.

The SBM graph was generated by creating 10 clusters with each node having uniform probability of belonging to a cluster. Edges between nodes were generated according to assigned intra- and inter-cluster probabilities. The edges generated were assigned weights from a Laplacian distribution with rate $\lambda_e = 2$. Finally, the matrix was normalized by 1.1 times its largest eigenvalue.

The ER graph was generated by taking edges from a standard normal $\mathcal{N}(0, 1)$ distribution and then thresholding edges to be between 1.6 and 1.8 in absolute to yield an effective probability of an edge $p_{ER} \approx 0.04$. The edges were soft thresholded by 1.5 to be between 0.1 and 0.3 in magnitude. Finally, the matrix was normalized by 1.5 times its largest eigenvalue.

The PL graph was generated by starting with a 15 node ER graph with connection probability 0.8. New nodes were connected by two new edges to and from an existing node of weight drawn as $\mathcal{N}(0, 1)$ and then offset 0.25 away from 0. The connections were made according to a modified preferential attachment scheme [34] in which the probability of the new node connecting to an existing node was proportional to the existing node's total weighted degree. The diagonal was set to $-1/2$. Lastly, the matrix was normalized by 1.5 times its largest eigenvalue.

Examples of these topologies with their weighted edges and representative estimates $\hat{\mathbf{A}}$ can be seen in figures 3 and 4 (higher absolute weights are displayed in darker blue). Some of these topologies are difficult to visualize for large numbers of nodes. For KR we used a circular layout in which the true edges are along the perimeter and not through the interior, for ER and SBM we used force-directed edge bundling [35] to

(a) Error in \mathbf{A} (left) and ϵ (right) for KR graph(b) Error in \mathbf{A} (left) and ϵ (right) for SBM graphFig. 5. Error in \mathbf{A} (left) and ϵ (right) for KR (top row) and SBM (bottom row) graphs for $N=1000$

group nearby edges into few thicker “strands”, and for PL we used a Fruchterman-Reingold [36] node positioning.

Once the \mathbf{A} matrix was generated with $N \in \{1000, 1500\}$ nodes, for fixed $M = 3$ the coefficients c_{ij} for $2 \geq i \leq M$ and $0 \leq j \leq i$ were generated sparsely from a mixture of uniform distributions $2^{i+j} c_{ij} \sim \frac{1}{2}\mathcal{U}(-1, -0.45) + \frac{1}{2}\mathcal{U}(0.45, 1)$ and normalized by 1.5 to correspond to a stable system.

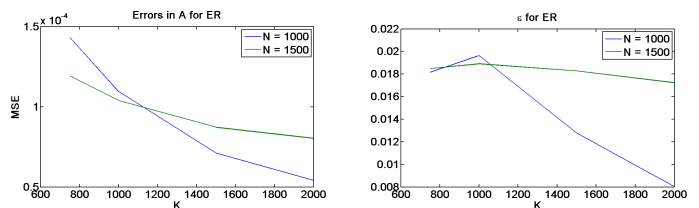
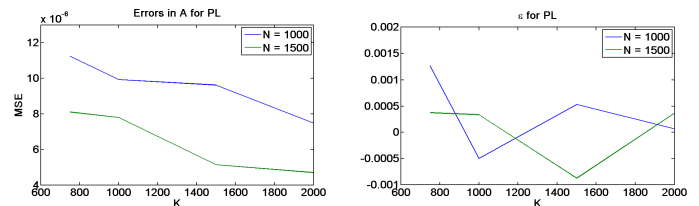
The data matrices \mathbf{X} were formed by generating random initial samples (with some burn in samples to reach steady state) and zero-mean unit-covariance additive white Gaussian noise $\mathbf{w}[k]$ computing $K \in \{750, 1000, 1500, 2000\}$ samples of $\mathbf{x}[k]$ according to (4). Then 20 such Monte-Carlo data matrices were generated independently, and $(\hat{\mathbf{A}}, \hat{\epsilon})$ was estimated using the simplified algorithm for varying values of λ and ρ . The average error of the \mathbf{A} matrix was computed as

$$MSE = \frac{1}{N^2} \|\mathbf{A} - \hat{\mathbf{A}}\|_F^2.$$

The empirical value of the error metric $\hat{\epsilon}$ from (21) was also measured by generating another 20 independent sets of timeseries z_k (as in (22) at steady state and using the estimates to predict the last sample using the first M).

In figure 5 and figure 6, we show the errors in \mathbf{A} and the empirical estimates of ϵ across the grid of λ and ρ . We performed the estimation on this grid and choose the lowest observed error to be $\hat{\epsilon}$. We see several different behaviors. In figure 5 we observe that the average errors in \mathbf{A} and empirical averages for ϵ for the KR graph are decreasing with both N and K . We observe similar behavior for the SBM graph, suggesting that graphs generating according to this topology might satisfy the assumptions in section VI. On the other hand in figure 6, the error in \mathbf{A} for ER does not display a clear trend in N , although observing more samples still improves the estimate of \mathbf{A} and the model prediction performance as expected. For the PL model, the error in estimating \mathbf{A} decreased with increasing N and K , but the error ϵ fluctuated around 0 with no clear trend.

This varied behavior arises because the different structured and random graph topologies examined tend to exhibit certain

(a) Error in \mathbf{A} (left) and ϵ (right) for ER graph(b) Error in \mathbf{A} (left) and ϵ (right) for PL graphFig. 6. Error in \mathbf{A} (left) and ϵ (right) for ER (top row) and PL (bottom row) graphs for $N=1000$

network properties that do not all correspond directly to the assumptions in section VI. In particular, the k -regular graph by its construction does satisfies the assumptions. This is because taking the n -th power of the adjacency matrix of a k -regular graph of this form results in an (nk) -regular graph, which satisfies the sparsity (A5) with some constants that do not grow too fast with N and K . Thus, the results of the KR graph empirically conforms to the predictions given by the theory in section VI. With the other topologies, the behavior of the sparsity constants is not as immediately clear, but the observed results suggest that some of the assumptions could be slightly loosened or that other network statistics (e.g., diameter or maximum degree) could play a role in the performance.

VIII. CONCLUSIONS

We have presented a new type of graph-based network process and several computationally tractable algorithms for estimating such causal networks. We have analyzed the statistical performance of one of these algorithms. We have demonstrated empirically that the model is competitive with previous models in describing real temperature sensor network timeseries with comparable levels of sparsity in their graphs or with comparable number of nonzero parameters. We have also shown through experiments that the simplified estimation algorithm presented is able to accurately estimate a sparse graph topology from data generated when the true timeseries is generated by this model.

REFERENCES

- [1] Matthew O. Jackson, *Social and Economic Networks*, Princeton University Press, Nov. 2010.
- [2] Kevin P. Murphy, Yair Weiss, and Michael I. Jordan, “Loopy Belief Propagation for Approximate Inference: An Empirical Study,” in *Proceedings of the Fifteenth Conference on Uncertainty in Artificial Intelligence*, San Francisco, CA, USA, 1999, UAI’99, pp. 467–475, Morgan Kaufmann Publishers Inc.
- [3] A. Sandryhaila and J. M. F. Moura, “Discrete Signal Processing on Graphs,” *IEEE Transactions on Signal Processing*, vol. 61, no. 7, pp. 1644–1656, Apr. 2013.

- [4] Mark Newman, *Networks: An Introduction*, Oxford University Press, Mar. 2010.
- [5] Sam T. Roweis and Lawrence K. Saul, “Nonlinear Dimensionality Reduction by Locally Linear Embedding,” *Science*, vol. 290, no. 5500, pp. 2323–2326, Dec. 2000.
- [6] Joshua B. Tenenbaum, Vin de Silva, and John C. Langford, “A Global Geometric Framework for Nonlinear Dimensionality Reduction,” *Science*, vol. 290, no. 5500, pp. 2319–2323, Dec. 2000.
- [7] N. Meinshausen and P. Bühlmann, “High-dimensional graphs and variable selection with the Lasso,” *Ann. Stat.*, vol. 34, no. 3, pp. 1436–1462, June 2006.
- [8] P. Ravikumar, M. J. Wainwright, G. Raskutti, and B. Yu, “High-dimensional covariance estimation by minimizing l_1 -penalized log-determinant divergence,” *Electronic Journal of Statistics*, vol. 5, pp. 935–980, 2011.
- [9] A. Bolstad, B.D. Van Veen, and R. Nowak, “Causal Network Inference Via Group Sparse Regularization,” *IEEE Transactions on Signal Processing*, vol. 59, no. 6, pp. 2628–2641, June 2011.
- [10] C. W. J. Granger, “Investigating Causal Relations by Econometric Models and Cross-spectral Methods,” *Econometrica*, vol. 37, no. 3, pp. 424–438, Aug. 1969.
- [11] A. Sandryhaila and J. M. F. Moura, “Discrete Signal Processing on Graphs: Frequency Analysis,” *IEEE Transactions on Signal Processing*, vol. 62, no. 12, pp. 3042–3054, June 2014.
- [12] Jerome Friedman, Trevor Hastie, and Robert Tibshirani, “Sparse inverse covariance estimation with the graphical Lasso,” *Biostatistics*, vol. 9, no. 3, pp. 432–441, July 2008.
- [13] Venkat Chandrasekaran, Pablo A. Parrilo, and Alan S. Willsky, “Latent variable graphical model selection via convex optimization,” *The Annals of Statistics*, vol. 40, no. 4, pp. 1935–1967, Aug. 2012.
- [14] F. R. Bach and M. I. Jordan, “Learning graphical models for stationary time series,” *IEEE Transactions on Signal Processing*, vol. 52, no. 8, pp. 2189–2199, Aug. 2004.
- [15] Jitkomut Songsiri and L. Vandenberghe, “Topology selection in graphical models of autoregressive processes,” *J. Mach. Learn. Res.*, vol. 11, pp. 2671–2705, 2010.
- [16] C. W. J. Granger, “Causality, cointegration, and control,” *J. of Econ. Dynamics and Control*, vol. 12, no. 2–3, pp. 551–559, June 1988.
- [17] C. W. J. Granger, “Some recent development in a concept of causality,” *Journal of Econometrics*, vol. 39, no. 1–2, pp. 199–211, Sept. 1988.
- [18] D.I. Shuman, S.K. Narang, P. Frossard, A. Ortega, and P. Vandergheynst, “The emerging field of signal processing on graphs: Extending high-dimensional data analysis to networks and other irregular domains,” *IEEE Signal Processing Magazine*, vol. 30, no. 3, pp. 83–98, May 2013.
- [19] David K. Hammond, Pierre Vandergheynst, and Rémi Gribonval, “Wavelets on graphs via spectral graph theory,” *Applied and Computational Harmonic Analysis*, vol. 30, no. 2, pp. 129–150, Mar. 2011.
- [20] R. R. Coifman and M. Maggioni, “Diffusion wavelets,” *Applied and Computational Harmonic Analysis*, vol. 21, no. 1, pp. 53–94, July 2006.
- [21] D. Thanou, D.I. Shuman, and P. Frossard, “Learning Parametric Dictionaries for Signals on Graphs,” *IEEE Transactions on Signal Processing*, vol. 62, no. 15, pp. 3849–3862, Aug. 2014.
- [22] G. M. Goerg and C. R. Shalizi, “LICORS: Light Cone Reconstruction of States for Non-parametric Forecasting of Spatio-Temporal Systems,” *arXiv:1206.2398 [physics, stat]*, June 2012, arXiv: 1206.2398.
- [23] A. Sandryhaila and J. M. F. Moura, “Big Data Analysis with Signal Processing on Graphs: Representation and processing of massive data sets with irregular structure,” *IEEE Signal Processing Magazine*, vol. 31, no. 5, pp. 80–90, Sept. 2014.
- [24] M.A.T. Figueiredo, R.D. Nowak, and S.J. Wright, “Gradient Projection for Sparse Reconstruction: Application to Compressed Sensing and Other Inverse Problems,” *IEEE Journal of Selected Topics in Signal Processing*, vol. 1, no. 4, pp. 586–597, Dec. 2007.
- [25] P. Tseng, “Convergence of a block coordinate descent method for nondifferentiable minimization,” *J. Optim Theory Appl.*, pp. 475–494, 2001.
- [26] D.P. Bertsekas, A. Nedić, and A.E. Ozdaglar, *Convex Analysis and Optimization*, Athena Scientific, 2003.
- [27] Sumanta Basu and George Michailidis, “Regularized estimation in sparse high-dimensional time series models,” *The Annals of Statistics*, vol. 43, no. 4, pp. 1535–1567, Aug. 2015.
- [28] Ravi Ganti, Nikhil Rao, Rebecca M. Willett, and Robert Nowak, “Learning Single Index Models in High Dimensions,” *arXiv:1506.08910 [cs, stat]*, June 2015, arXiv: 1506.08910.
- [29] M. Schmidt, G. Fung, and R. Rosales, “Fast Optimization Methods for l_1 Regularization: A Comparative Study and Two New Approaches,” in *Machine Learning: ECML 2007*, pp. 286–297. Springer, Sept. 2007.
- [30] B. O’Donoghue and E. Candès, “Adaptive Restart for Accelerated Gradient Schemes,” *Foundations of Computational Mathematics*, vol. 15, no. 3, pp. 715–732, July 2013.
- [31] “National Climactic Data Center,” <ftp://ftp.ncdc.noaa.gov/pub/data/gsoad>, 2011.
- [32] B. Karrer and M. E. J. Newman, “Stochastic blockmodels and community structure in networks,” *Physical Review. E, Statistical, Nonlinear, and Soft Matter Physics*, vol. 83, no. 1 Pt 2, pp. 016107, Jan. 2011.
- [33] P. Erdős and A. Rényi, “On the Evolution of Random Graphs,” in *Publication of the Mathematical Institute of the Hungarian Academy of Sciences*, 1960, pp. 17–61.
- [34] A. Barabási and R. Albert, “Emergence of Scaling in Random Networks,” *Science*, vol. 286, no. 5439, pp. 509–512, Oct. 1999.
- [35] Danny Holten and Jarke J. Van Wijk, “Force-Directed Edge Bundling for Graph Visualization,” *Computer Graphics Forum*, vol. 28, no. 3, pp. 983–990, June 2009.
- [36] Thomas M. J. Fruchterman and Edward M. Reingold, “Graph drawing by force-directed placement,” *Software: Practice and Experience*, vol. 21, no. 11, pp. 1129–1164, Nov. 1991.
- [37] Iain M. Johnstone, “Chi-square oracle inequalities,” in *Institute of Mathematical Statistics Lecture Notes - Monograph Series*, pp. 399–418. Institute of Mathematical Statistics, Beachwood, OH, 2001.
- [38] David G. Feingold and Richard Varga, “Block diagonally dominant matrices and generalizations of the Gerschgorin circle theorem,” *Pacific Journal of Mathematics*, vol. 12, no. 4, pp. 1241–1250, Dec. 1962.

APPENDIX A PROOF OF LEMMA 1

We introduce preliminary notation used to describe “stability” of systems taken from [27], which are used in the proof, and also give the forms for ω and $\mu_{\min}(\tilde{\mathcal{A}})$.

Let the z-transforms for a CGP system be given

$$\mathcal{A}(z) = \mathbf{I} - z\mathbf{A} - z^2 P_2(\mathbf{A}, \mathbf{c}) - \dots - z^M P_M(\mathbf{A}, \mathbf{c})$$

and similarly let $\tilde{\mathcal{A}}(z) = \mathbf{I} - z\tilde{\mathbf{A}}_0$ where

$$\tilde{\mathbf{A}}_0 = \begin{pmatrix} \mathbf{A} & P_2(\mathbf{A}, \mathbf{c}) & \dots & P_{M-1}(\mathbf{A}, \mathbf{c}) & P_M(\mathbf{A}, \mathbf{c}) \\ \mathbf{I}_N & & & \mathbf{0} & \mathbf{0} \\ & \mathbf{I}_N & & & \mathbf{0} \\ & & \ddots & & \vdots \\ \mathbf{0} & & & \mathbf{I}_N & \mathbf{0} \end{pmatrix}$$

is the $NM \times NM$ block companion matrix of the autoregressive process.

Using the z-transforms, we define measures of stability,

$$\mu_{\min}(\mathcal{A}) = \min_{|z|=1} \Lambda_{\min}(\mathcal{A}^*(z)\mathcal{A}(z))$$

$$\mu_{\max}(\mathcal{A}) = \max_{|z|=1} \Lambda_{\max}(\mathcal{A}^*(z)\mathcal{A}(z))$$

where $\Lambda_{\min/\max}(\cdot)$ denotes the smallest/largest eigenvalue of its matrix argument.

Proof of Lemma 1. To use Propositions 4.1-4.3 from [27], we bound the quantities $\mu_{\min/\max}(\mathcal{A})$. Let $\mathcal{B}(z) = \mathbf{I} - \mathcal{A}(z)$ and similarly $\tilde{\mathcal{B}}(z) = \mathbf{I} - \tilde{\mathcal{A}}(z)$.

$$\begin{aligned} \sqrt{\mu_{\max}(\mathcal{A})} &\leq \max_{|z|=1} \|\mathbf{I} - \mathcal{B}(z)\| \\ &\leq 1 + \sum_{i=2}^M \max_{|z|=1} |z^i| \|P_i(\mathbf{A}, \mathbf{c})\| \\ &\leq 1 + L + \sum_{i=2}^M \sum_{j=0}^i |c_{ij}| \|\mathbf{A}^j\| \\ &\leq 1 + L + L \sum_{i=2}^M \sum_{j=1}^i |c_{ij}| + \sum_{i=2}^M |c_{i0}| \\ &\leq (1 + L + L\rho + \rho) = Q \end{aligned} \tag{25}$$

by assumption **(A5)**, and similarly

$$\begin{aligned} \sqrt{\mu_{\min}(\mathcal{A})} &\geq \min_{|z|=1} \left\| (\mathbf{I} - \mathcal{B}(z))^{-1} \right\|^{-1} \\ &\stackrel{(a)}{\geq} 1 - \max_{|z|=1} \|\mathcal{B}(z)\| \geq 2 - Q \end{aligned}$$

where the inequality marked (a) is due to assumption **(A5)** and the rest follows from similar logic as (25). Propositions 4.2-4.3 hold w.h.p. when $T \geq d_0 s_{MN} \tilde{\omega}^2 (\log M + \log N)$, where $\omega \geq \tilde{\omega} = \frac{\|\Sigma_{\mathbf{w}}\|}{\|\Sigma_{\mathbf{w}}^{-1}\|^{-1}} \frac{\mu_{\max}(\mathcal{A})}{\mu_{\min}(\mathcal{A})}$. Thus, when assumption **(A6)** holds, this condition is satisfied as well. Finally, we substitute these upper and lower bounds for $\mu_{\min}/\mu_{\max}(\mathcal{A})$ into the statements of Proposition 4.1 to yield the statement of theorem 4. \square

APPENDIX B PROOF OF LEMMA 2

Proof. First, note that $\mathbb{E}[\mathbf{x}^\top \mathbf{B} \mathbf{x}] = \text{tr}(\mathbf{B})$. Now let $f(\mathbf{B}) = \mathbf{x}^\top \mathbf{B} \mathbf{x} - \text{tr}(\mathbf{B})$. We have the gradient $\frac{df(\mathbf{B})}{d\mathbf{B}} = \mathbf{x} \mathbf{x}^\top - \mathbf{I}_n$, which is a constant with respect to \mathbf{B} . Then the value of $\mathbf{B}^* \in \mathcal{B}$ that maximizes $f(\mathbf{B})$ is at the boundary of the set \mathcal{B} in the direction of the gradient, $\mathbf{B}^* = \frac{J}{\|\mathbf{x} \mathbf{x}^\top - \mathbf{I}_n\|} (\mathbf{x} \mathbf{x}^\top - \mathbf{I}_n)$. Since $\mathbf{x} \mathbf{x}^\top$ has rank 1 and $\|\mathbf{I}_n\| = 1$, we can see that $\|\mathbf{x} \mathbf{x}^\top - \mathbf{I}_n\| = \max(|\mathbf{x}^\top \mathbf{x} - 1|, 1)$. Then

$$\begin{aligned} &\sup_{\mathbf{B} \in \mathcal{B}} (\mathbf{x}^\top \mathbf{B} \mathbf{x} - \mathbb{E}[\mathbf{x}^\top \mathbf{B} \mathbf{x}]) \\ &= \frac{J}{\max(|\mathbf{x}^\top \mathbf{x} - 1|, 1)} (\mathbf{x}^\top (\mathbf{x} \mathbf{x}^\top - \mathbf{I}_n) \mathbf{x} - \text{tr}(\mathbf{x} \mathbf{x}^\top - \mathbf{I}_n)) \\ &= \frac{J}{\max(|z - 1|, 1)} (z^2 - 2z + n) \end{aligned}$$

where $z = \mathbf{x}^\top \mathbf{x} \sim \chi_n^2$ is a Chi-squared random variable with n degrees of freedom. We can see similarly that

$$\sup_{\mathbf{B} \in \mathcal{B}} (\mathbb{E}[\mathbf{x}^\top \mathbf{B} \mathbf{x}] - \mathbf{x}^\top \mathbf{B} \mathbf{x}) = \frac{J}{\max(|z - 1|, 1)} (z^2 - 2z + n)$$

which is the same expression, so our analysis will produce a bound for both directions.

Now consider the set

$$\begin{aligned} &\left[\frac{J}{\max(|z - 1|, 1)} (z^2 - 2z + n) \geq t \right] \\ &= \left[\left((z^2 - 2z + n) \geq \frac{t}{J} \right) \cap (|z - 1| \leq 1) \right] \\ &\quad \cup \left[\left((z^2 - 2z + n) \geq \frac{t}{J} |z - 1| \right) \cap (|z - 1| \geq 1) \right] \end{aligned} \quad (26)$$

Note that since $z \geq 0$ w.p.1, we can consider the equivalent sets $\{|z - 1| \leq 1\} = \{z \leq 2\}$ and $\{|z - 1| \geq 1\} = \{z \geq 2\}$. We manipulate the probability,

$$\begin{aligned} &P \left(\sup_{\mathbf{B} \in \mathcal{B}} (\mathbf{x}^\top \mathbf{B} \mathbf{x} - \mathbb{E}[\mathbf{x}^\top \mathbf{B} \mathbf{x}]) > t \right) \\ &= P \left(\left[\left((z^2 - 2z + n) \geq \frac{t}{J} \right) \cap (z \leq 2) \right] \right. \\ &\quad \left. \cup \left[\left((z^2 - 2z + n) \geq \frac{t}{J} |z - 1| \right) \cap (z \geq 2) \right] \right) \\ &\stackrel{(a)}{\leq} P \left(\left((z^2 - 2z + n) \geq \frac{t}{J} \right) \cap (z \leq 2) \right) \\ &\quad + P \left(\left((z^2 - 2z + n) \geq \frac{t}{J} (z - 1) \right) \cap (z \geq 2) \right) \\ &\leq P(z \leq 2) + P \left(z^2 - 2z + n \geq \frac{t}{J} (z - 1) \right) \end{aligned}$$

$$\begin{aligned} &\stackrel{(b)}{=} P(z \leq 2) \\ &\quad + P \left(z \geq \frac{1}{2} \left(2 + \frac{t}{J} + \sqrt{\left(2 + \frac{t}{J} \right)^2 + 4 \left(\frac{t}{J} + n \right)^2} \right) \right) \\ &\stackrel{(c)}{\leq} \frac{1}{e} \left(\frac{2e}{n} \right)^{n/2} + P \left(z \geq \frac{1}{2} \left(2 + \frac{t}{J} + 2 \left(\frac{t}{J} + n \right) \right) \right) \\ &= \frac{1}{e} \left(\frac{2e}{n} \right)^{n/2} + P \left(z - n \geq 1 + \frac{3t}{2J} \right) \\ &\stackrel{(d)}{\leq} \frac{1}{e} \left(\frac{2e}{n} \right)^{n/2} + \exp \left\{ -\frac{27}{64} \frac{t^2}{J^2 n} \right\} \end{aligned}$$

where inequality (a) is implied by $z \geq 2 \Rightarrow |z - 1| = z - 1$. In inequality (b), we drop the second term of the quadratic inequality since $\frac{1}{2} \left(2 + \frac{t}{J} - \sqrt{\left(2 + \frac{t}{J} \right)^2 + 4 \left(\frac{t}{J} + n \right)^2} \right) < 0$. In (c) we use a bound on chi-squared variables [37] for the first term. Finally, with another application of a second bound on chi-squared variables in (d), we have the result. \square

APPENDIX C PROOF OF LEMMA 3

Before we start the proof, we state a corollary to Lemma 2,

Corollary 2.1. *Using the same notations as Lemma 2, by taking $t = J(n^{1/2+\beta/2})/3$ with $0 \leq \beta \leq 1$, for all $\mathbf{B}' \in \mathcal{B}$ (that are not necessarily fixed and can depend on \mathbf{x})*

$$\begin{aligned} &P \left(\frac{1}{n} \mathbf{x}^\top \mathbf{B}' \mathbf{x} > \frac{1}{n} \mathbb{E}[\mathbf{x}^\top \mathbf{B}' \mathbf{x}] + J n^{(\beta-1)/2} \right) \leq \gamma \\ &P \left(\frac{1}{n} \mathbf{x}^\top \mathbf{B}' \mathbf{x} < \frac{1}{n} \mathbb{E}[\mathbf{x}^\top \mathbf{B}' \mathbf{x}] - J n^{(\beta-1)/2} \right) \leq \gamma \end{aligned} \quad (27)$$

where $\gamma = \frac{1}{e} \left(\frac{2e}{n} \right)^{n/2} + \exp \left\{ -\frac{3}{64} n^\beta \right\}$

Proof of Lemma 3. Let $g(\mathbf{c}', \mathbf{z}_k) = \|\mathbf{x}[k] - f(\tilde{\mathbf{A}}, \mathbf{c}', \mathbf{X}_{k-1})\|_2^2$ and $\tilde{\mu}_k = \mathbb{E}[g(\tilde{\mathbf{c}}, \mathbf{z}_k)]$. Note we can rewrite

$$\begin{aligned} &\sum_{k=M}^{K-1} g(\tilde{\mathbf{c}}, \mathbf{z}_k) = \mathbf{x}_{0:K-1}^\top \mathbf{B}' \mathbf{x}_{0:K-1} \\ &\text{where } \mathbf{B}' = \sum_{k=0}^{T-1} (\mathbf{B} \mathbf{P}^k)^\top \mathbf{B} \mathbf{P}^k, \\ &\mathbf{B} = \underbrace{(\mathbf{I}_N \quad -P_1(\mathbf{A}, \mathbf{c}) \quad -P_2(\mathbf{A}, \mathbf{c}) \quad \dots \quad -P_M(\mathbf{A}, \mathbf{c}) \quad \mathbf{0}_N \quad \dots \quad \mathbf{0}_N)}_{\substack{M+1 \text{ blocks} \\ T-1 \text{ times}}} \end{aligned}$$

permutation matrix, and $\mathbf{x}_{0:K-1}$ is a stacked vector containing all observed data.

Note that \mathbf{B}' is a symmetric block banded matrix. Then, we have by an extension of Gershgorin's circle theorem to block matrices [38] that

$\|\mathbf{B}'\| \leq (\|\mathbf{I}_N\| + \|P_1(\mathbf{A}, \mathbf{c})\| + \dots + \|P_M(\mathbf{A}, \mathbf{c})\|) \leq Q^2$ by **(A5)** and reasoning similar to (25). Now, let the whitened data vector $\tilde{\mathbf{x}} = \tilde{\Sigma}^{-1/2} \mathbf{x}_{0:K-1}$ where $\tilde{\Sigma}^{-1/2}$ is the inverse matrix square root of $\mathbb{E}[\mathbf{x}_{0:K-1} \mathbf{x}_{0:K-1}^\top]$, so that $\sum_{k=M}^{K-1} g(\tilde{\mathbf{c}}, \mathbf{z}_k) = \tilde{\mathbf{x}}^\top \tilde{\Sigma}^{1/2} \mathbf{B}' \tilde{\Sigma}^{-1/2} \tilde{\mathbf{x}}$. By another application of Gershgorin's circle theorem, we have that $\|\tilde{\Sigma}\| \leq \sum_{i=-\infty}^{\infty} \|\mathbb{E}[\mathbf{x}[k] \mathbf{x}[k - i]^\top]\| = G$. Then $\|\tilde{\Sigma}^{1/2} \mathbf{B}' \tilde{\Sigma}^{1/2}\| \leq \|\mathbf{B}'\| \|\tilde{\Sigma}\| = GQ^2$

Now applying Lemma 2,

$$P\left(\frac{1}{NK} \sum_{k=M}^{K-1} (g(\tilde{\mathbf{c}}, \mathbf{z}_k) - \tilde{\mu}_k) \leq -\frac{GQ^2}{(NK)^{(1-\beta)/2}}\right) \leq \gamma.$$

Similarly,

$$P\left(\frac{1}{NK} \sum_{k=M}^{K-1} (g(\mathbf{c}, \mathbf{z}_k) - \mu_k) \geq \frac{GQ^2}{(NK)^{(1-\beta)/2}}\right) \leq \gamma.$$

Then with some algebra and the union bound,

$$\begin{aligned} & P\left(\frac{1}{N} (\tilde{\mu}_k - \mu_k) \geq \frac{1}{NT} \sum_{k=M}^{K-1} (g(\tilde{\mathbf{c}}, \mathbf{z}_k) - g(\mathbf{c}, \mathbf{z}_k)) \right. \\ & \quad \left. + \frac{2GQ^2K}{T(NK)^{(1-\beta)/2}}\right) \\ &= P\left(\frac{1}{NK} \sum_{k=M}^{K-1} (g(\mathbf{c}, \mathbf{z}_k) - \mu_k) \right. \\ & \quad \left. - \frac{1}{NK} \sum_{k=M}^{K-1} (g(\tilde{\mathbf{c}}, \mathbf{z}_k) - \tilde{\mu}_k) \geq \frac{2GQ^2}{(NK)^{(1-\beta)/2}}\right) \\ &\leq P\left(\left[\frac{1}{NK} \sum_{k=M}^{K-1} (g(\tilde{\mathbf{c}}, \mathbf{z}_k) - \tilde{\mu}_k) \leq -\frac{GQ^2}{(NK)^{(1-\beta)/2}}\right] \right. \\ & \quad \left. \cup \left[\frac{1}{NK} \sum_{k=M}^{K-1} (g(\mathbf{c}, \mathbf{z}_k) - \mu_k) \geq \frac{GQ^2}{(NK)^{(1-\beta)/2}}\right]\right) \\ &\leq 2\gamma \end{aligned}$$

APPENDIX D

PROOF OF THEOREM 4

Proof. The excess risk can be bounded as

$$\begin{aligned} N\epsilon &= \mathbb{E} \left[\left\| \mathbf{x}[k] - f(\tilde{\mathbf{A}}, \tilde{\mathbf{c}}, \mathbf{X}_{k-1}) \right\|_2^2 \right] \\ &\quad - \mathbb{E} \left[\left\| \mathbf{x}[k] - f(\mathbf{A}, \mathbf{c}, \mathbf{X}_{k-1}) \right\|_2^2 \right] \\ &= \mathbb{E} \left[\left\| \mathbf{x}[k] - f(\tilde{\mathbf{A}}, \tilde{\mathbf{c}}, \mathbf{X}_{k-1}) \right\|_2^2 \right] \\ &\quad - \mathbb{E} \left[\left\| \mathbf{x}[k] - f(\tilde{\mathbf{A}}, \mathbf{c}, \mathbf{X}_{k-1}) \right\|_2^2 \right] \\ &\quad + \mathbb{E} \left[\left\| f(\tilde{\mathbf{A}}, \mathbf{c}, \mathbf{X}_{k-1}) - f(\mathbf{A}, \mathbf{c}, \mathbf{X}_{k-1}) \right\|_2^2 \right] \\ &\stackrel{(a)}{=} NV_1 - \mathbb{E} \left[\left\| f(\tilde{\mathbf{A}}, \mathbf{c}, \mathbf{X}_{k-1}) - f(\mathbf{A}, \mathbf{c}, \mathbf{X}_{k-1}) \right\|_2^2 \right] \\ &\quad - 2 \mathbb{E} \left[\left(\mathbf{x}[k] - f(\tilde{\mathbf{A}}, \mathbf{c}, \mathbf{X}_{k-1}) \right)^\top \right. \\ &\quad \quad \left. \left(f(\tilde{\mathbf{A}}, \mathbf{c}, \mathbf{X}_{k-1}) - f(\mathbf{A}, \mathbf{c}, \mathbf{X}_{k-1}) \right) \right] \\ &= NV_1 - \mathbb{E} \left[\left\| f(\tilde{\mathbf{A}}, \mathbf{c}, \mathbf{X}_{k-1}) - f(\mathbf{A}, \mathbf{c}, \mathbf{X}_{k-1}) \right\|_2^2 \right] \\ &\quad - 2 \mathbb{E} \left[\left(\mathbf{x}[k] - f(\mathbf{A}, \mathbf{c}, \mathbf{X}_{k-1}) \right) \right. \\ &\quad \quad \left. + f(\mathbf{A}, \mathbf{c}, \mathbf{X}_{k-1}) - f(\tilde{\mathbf{A}}, \mathbf{c}, \mathbf{X}_{k-1}) \right)^\top \\ &\quad \quad \left. \left(f(\tilde{\mathbf{A}}, \mathbf{c}, \mathbf{X}_{k-1}) - f(\mathbf{A}, \mathbf{c}, \mathbf{X}_{k-1}) \right) \right] \\ &= NV_1 + \mathbb{E} \left[\left\| f(\tilde{\mathbf{A}}, \mathbf{c}, \mathbf{X}_{k-1}) - f(\mathbf{A}, \mathbf{c}, \mathbf{X}_{k-1}) \right\|_2^2 \right] \\ &\quad - 2 \mathbb{E} \left[\left(\mathbf{x}[k] - f(\mathbf{A}, \mathbf{c}, \mathbf{X}_{k-1}) \right)^\top \right. \\ &\quad \quad \left. \left(f(\tilde{\mathbf{A}}, \mathbf{c}, \mathbf{X}_{k-1}) - f(\mathbf{A}, \mathbf{c}, \mathbf{X}_{k-1}) \right) \right] \\ &\Rightarrow \epsilon \stackrel{(b)}{=} V_1 + \underbrace{\frac{1}{N} \mathbb{E} \left[\left\| f(\tilde{\mathbf{A}}, \mathbf{c}, \mathbf{X}_{k-1}) - f(\mathbf{A}, \mathbf{c}, \mathbf{X}_{k-1}) \right\|_2^2 \right]}_{V_2} \end{aligned}$$

where in equation (a) we set

$V_1 = \mathbb{E} \left[\left\| \mathbf{x}[k] - f(\tilde{\mathbf{A}}, \tilde{\mathbf{c}}, \mathbf{X}_{k-1}) \right\|_2^2 \right] - \mathbb{E} \left[\left\| \mathbf{x}[k] - f(\tilde{\mathbf{A}}, \mathbf{c}, \mathbf{X}_{k-1}) \right\|_2^2 \right]$ and we arrive at equation (b) because $\mathbb{E} \left[(\mathbf{x}[k] - f(\mathbf{A}, \mathbf{c}, \mathbf{X}_{k-1}))^\top (f(\tilde{\mathbf{A}}, \mathbf{c}, \mathbf{X}_{k-1}) - f(\mathbf{A}, \mathbf{c}, \mathbf{X}_{k-1})) \right] = 0$ which is due to $\mathbf{w}[k] = \mathbf{x}[k] - f(\mathbf{A}, \mathbf{c}, \mathbf{X}_{k-1})$ being uncorrelated with (or independent of) $\mathbf{x}[j]$ for $j \leq k$.

Now the terms V_1 and V_2 need to be bounded. To bound V_1 , we invoke Lemma 3,

$$\begin{aligned} V_1 &\leq \frac{1}{NT} \sum_{k=M}^{K-1} \left(\left\| \mathbf{x}[k] - f(\tilde{\mathbf{A}}, \tilde{\mathbf{c}}, \mathbf{X}_{k-1}) \right\|_2^2 \right. \\ &\quad \left. - \left\| \mathbf{x}[k] - f(\tilde{\mathbf{A}}, \mathbf{c}, \mathbf{X}_{k-1}) \right\|_2^2 \right) + \frac{2GQ^2K}{T(NK)^{(1-\beta)/2}} \\ &\Rightarrow V_1 \leq \frac{2GQ^2K}{T(NK)^{(1-\beta)/2}} \quad \text{w.h.p.} \end{aligned}$$

which follows since the term in parentheses is negative because $\tilde{\mathbf{c}}$ minimizes the first term via the optimization problem (13), and by Assumption (A5), $\|\tilde{\mathbf{c}}\|_1 \leq \rho$ is a feasible point.

To bound V_2 , we first rewrite the expression,

$$\begin{aligned} & f(\tilde{\mathbf{A}}, \mathbf{c}, \mathbf{X}_{k-1}) - f(\mathbf{A}, \mathbf{c}, \mathbf{X}_{k-1}) \\ &= \left(\tilde{\Delta}_1 \quad c_{21}\tilde{\Delta}_1 + c_{22}\tilde{\Delta}_2 \quad \dots \quad \sum_{i=1}^M c_{Mi}\tilde{\Delta}_i \right) \mathbf{X}_{k-1} \end{aligned}$$

$$\Rightarrow \left\| f(\tilde{\mathbf{A}}, \mathbf{c}, \mathbf{X}_{k-1}) - f(\mathbf{A}, \mathbf{c}, \mathbf{X}_{k-1}) \right\|_2^2 \leq \left\| \left(\tilde{\mathbf{c}}^\top \otimes (\tilde{\mathbf{A}} - \mathbf{A}) \right) \mathbf{X}_{k-1} \right\|_2^2$$

where $\tilde{\Delta}_i = \tilde{\mathbf{A}}^i - \mathbf{A}^i$, $\Delta = \|\tilde{\mathbf{A}} - \mathbf{A}\|$,

$$\tilde{\mathbf{c}} = \left(1 \quad c_{21} + c_{22}(2\|\mathbf{A}\| + \Delta) \quad \dots \quad \sum_{i=1}^M c_{Mi} \frac{(\|\mathbf{A}\| + \Delta)^i - \|\mathbf{A}\|^i}{\Delta} \right)^\top$$

and \otimes denotes the kronecker (or tensor) product. Now, letting

$$\tilde{L}_M(\delta) = \max_{1 \leq i \leq M} \frac{(L + \delta)^i - L^i}{\delta}$$

and doing some algebra, we use Lemma 1,

$$\begin{aligned} NV_2 &= \mathbb{E} \left[\mathbf{X}_{k-1}^\top \left(\tilde{\mathbf{c}}^\top \otimes (\tilde{\mathbf{A}} - \mathbf{A}) \right)^\top \left(\tilde{\mathbf{c}}^\top \otimes (\tilde{\mathbf{A}} - \mathbf{A}) \right) \mathbf{X}_{k-1} \right] \\ &= \mathbb{E} \left[\sum_{i=1}^M \tilde{c}_i^2 \left\| (\tilde{\mathbf{A}} - \mathbf{A}) \mathbf{x}[k-i] \right\|_2^2 \right] \\ &= \mathbb{E} \left[\left\| (\tilde{\mathbf{A}} - \mathbf{A}) \mathbf{x}[k] \right\|_2^2 \sum_{i=1}^M \tilde{c}_i^2 \right] \\ &\leq \|\tilde{\mathbf{c}}\|_1^2 \left(\tilde{L}_M(\Delta) \right)^2 \|\tilde{\mathbf{A}} - \mathbf{A}\|_2^2 \text{tr}(\Sigma_0) \\ &\leq d_1 L^2 \delta^2 \left(\tilde{L}_M(\delta) \right)^2 \text{tr}(\Sigma_0) \quad \text{w.h.p} \end{aligned}$$

where $\delta^2 = \frac{\log M + \log N}{T} \frac{\sigma_u^2}{\sigma_\ell^2} Q^4 (g(Q))^2 s_{MN}$. Finally, we have by an application of the union bound,

$$\begin{aligned} P(\epsilon = V_1 + V_2 \geq \frac{2GQ^2K}{T(NK)^{(1-\beta)/2}} \\ + d_1 \frac{L^2 \delta^2}{N} \left(\tilde{L}_M(\delta) \right)^2 \text{tr}(\Sigma_0)) \\ \leq 2 \left(\frac{1}{e} \left(\frac{2e}{NK} \right)^{\frac{NK}{2}} + \exp \left\{ -\frac{3}{64} (NK)^\beta \right\} \right) \\ + d_2 \exp(-d_3 K) \\ \Rightarrow \epsilon \leq \frac{2GQ^2K}{T(NK)^{(1-\beta)/2}} + d_1 \frac{L^2 \delta^2}{N} \left(\tilde{L}_M(\delta) \right)^2 \text{tr}(\Sigma_0) \quad \text{w.h.p} \end{aligned}$$

for some $d_i > 0$. \square